

A review of coupling mechanism designs for modular reconfigurable robots

Wael Saab, Peter Racioppo and Pinhas Ben-Tzvi*

Robotics and Mechatronics Laboratory, Department of Mechanical Engineering, Virginia Tech, Blacksburg, VA 24061, USA. E-mails: waelsaab@vt.edu, rpeter8@vt.edu

(Accepted September 17, 2018. First published online: October 11, 2018)

SUMMARY

With the increasing demands for versatile robotic platforms capable of performing a variety of tasks in diverse and uncertain environments, the needs for adaptable robotic structures have been on the rise. These requirements have led to the development of modular reconfigurable robotic systems that are composed of a numerous self-sufficient modules. Each module is capable of establishing rigid connections between multiple modules to form new structures that enable new functionalities. This allows the system to adapt to unknown tasks and environments. In such structures, coupling between modules is of crucial importance to the overall functionality of the system. Over the last two decades, researchers in the field of modular reconfigurable robotics have developed novel coupling mechanisms intended to establish rigid and robust connections, while enhancing system autonomy and reconfigurability. In this paper, we review research contributions related to robotic coupling mechanism designs, with the aim of outlining current progress and identifying key challenges and opportunities that lay ahead. By presenting notable design approaches to coupling mechanisms and the most relevant efforts at addressing the challenges of sensorization, misalignment tolerance, and autonomous reconfiguration, we hope to provide a useful starting point for further research into the field of modular reconfigurable robotics and other applications of robotic coupling.

KEYWORDS: Robotic self-diagnosis and self-repair, Modular robotics, Swarm robotics, Multi-agent robot teams, Sensor network

1. Introduction

1.1. Background

Coupling between mechanical components is a basic task performed in a variety of engineered systems that enables a structure to fulfill multiple roles. Manually operated coupling may be as simple as connecting a socket to a wrench or as complex as remotely guiding a spacecraft to couple with an orbiting satellite. Autonomous coupling, on the other hand, requires advanced sensing and control schemes. In both scenarios, positional and rotational alignment requires high accuracy, and the established connection must sustain operational loads to ensure reliability. Additional considerations for coupling are the compatibility of the connectors, the energy required to maintain the connection, the ability to tolerate misalignment, and the ability to disconnect in the presence of a failure.

To simplify the coupling procedure, engineers can sometimes create ideal operating conditions in structured environments, as, for example, in the coupling of locomotive trains on a railroad. The dimensions of the rails and the trains are specified by universal standards to ensure uniformity and compatibility among the coupling interfaces. These interfaces consist of genderless hooks, held loosely enough that connections can be made at many orientations despite the accumulation of manufacturing and assembly errors. However, in unstructured environments, where the terrain and operating conditions may not be completely known *a priori*, the complexity of a coupling task

* Corresponding author: E-mail: bentzvi@vt.edu.

increases significantly. Autonomous coupling is further complicated by the requirement of sensory feedback and guidance algorithms for alignment.

The field of modular reconfigurable robotics relies on successful demonstration of self-reconfiguration, sometimes referred to as shape metamorphosis. This is a process in which multiple modules communicate, align in close proximity, and couple, forming rigid connections that enable new structures and capabilities.¹ Coupling of modular reconfigurable robots can be divided into two main categories: intra-robot coupling and inter-robot coupling.² Intra-robot coupling takes place between modules that are in a connected group, while inter-robot coupling occurs between independent and unconnected groups. Examples of intra-robot coupling include water flow movement of lattice-based structures or a chain-based structure that can reconfigure from a legged robot to a rolling ball or to a gripper. Inter-robot coupling includes situations where multiple modules aggregate, couple, and reconfigure to perform synchronized tasks, and disassemble back into independent modules as needed. In either category, the resultant coupled configuration enables the scaled formation to exhibit behaviors and accomplish tasks that would otherwise be impossible to achieve with a single module.

Modular reconfigurable robots exhibit a higher level of versatility and robustness, and can be constructed with lower production costs in comparison to conventional single structured robots.³ However, one of the main challenges, outlined in a review of modular reconfigurable robots by the authors in ref. [4] is designing reliable coupling mechanisms that can aid the self-reconfiguration procedure.

1.2. Motivation

The objective of this paper is to present, analyze, and compare research contributions made to robotic coupling mechanism design and technologies. This paper addresses general design considerations for coupling mechanisms, as well as reviews their implementation on modular self-reconfigurable robotic platforms. While there are many examples of manually connected coupling mechanisms, this review will focus on active mechanisms that enable autonomous connection and disconnection between robotic modules. The paper further assesses aspects of electrical design, sensorization, power and data sharing capabilities, module locomotion, and intelligent algorithms used to guide the coupling procedure. The objective is to summarize the most recent and relevant advances in the field and to formulate a general outline of the current state of coupling technology. It should be noted, however, that although coupling mechanisms have been proposed for applications such as hard or soft docking of spacecraft^{5,6} and unmanned underwater vehicles,^{7,8} our discussion will focus principally on direct applications to modular reconfigurable robots.

2. Design Attributes

This section introduces the key design attributes and terminology used to describe coupling mechanisms. The review of existing literature and comparative analysis, presented in Sections 4, 5, and 6 will refer to them to define the means of operation for mechanisms on board a range of modular robots.

2.1. Gender

The gender of choice for a coupling mechanism is strongly related to its mechanical design and directly influences the reconfigurability of the system. Figure 1(A) depicts an example of gendered coupling mechanisms that consists of a male and female connector. To establish a connection, a projection at one interface actively couples with an opposing passive interface. These types of coupling mechanisms are simple, but if the active interface malfunctions, the modules will not be able to disengage from the connection.

Bi-gendered coupling interfaces, as shown in Fig. 1(B), combine both male and female connectors into a single surface, resulting in a connection between two anti-symmetric interfaces.⁹ In a bi-gendered connection, both sides incorporate active elements that can be used to engage and disengage. These types of mechanisms eliminate the constraints of gendered connections during the reconfiguration process and enable two modules to connect at any pair of coupling locations, at the cost of increased design complexity.

A sub-category of the bi-gendered category is the so-called genderless coupling, which is defined by anti-symmetric interfaces that combine both male and female characteristics into especially

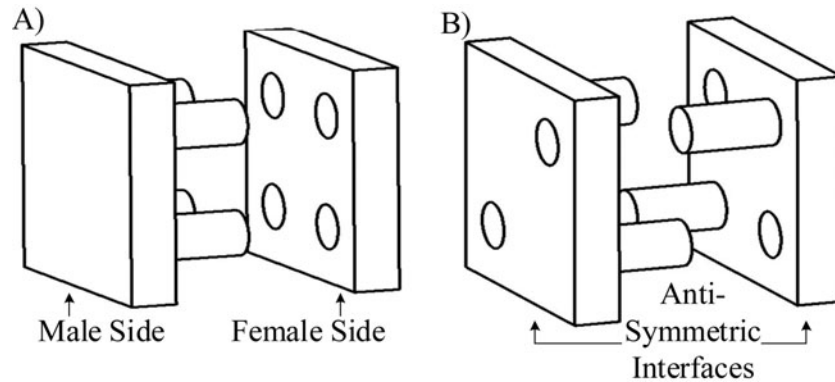


Fig. 1. Gender interface categories: (A) Gendered and (B) Bi-gendered.

designed connectors. The distinction between genderless and bi-gendered coupling comes from the implementation of the actuation. In a bi-gendered mechanism, both interfaces must be actuated to disconnect the modules. Conversely, genderless mechanisms can disconnect by actuating only one side of the coupling mechanism. These types of connections are classified as failsafe. Failsafe, genderless mechanisms have the distinct advantage of enabling modules to disconnect from disabled modules in a coupled state; a process termed self-repair.¹⁰ Genderless mechanisms are the most versatile of the three gender types, but require the most intricate mechanical design. The geometry of these connectors will be discussed in more detail in Section 4.

2.2. Actuation

The most common actuation methods for coupling mechanisms include motors, electro/permanent magnets, and Shape Memory Alloy (SMA) wire. The determining factor for actuation type is typically the size of the modular robot. The predominant forms of actuation for macro-sized modular robots are geared motors. They provide significant torque to lock the mating surfaces in place, and in some designs, provide relative rotation between two mechanically coupled modules. Non-back drivable transmission systems are preferred in such applications to maintain an established connection without constantly consuming power. While geared motors are useful for high-payload applications, they are not applicable for micro-scale coupling mechanisms. Electromagnets and SMA wire are the preferred means of actuation for miniaturized applications. Electromagnets are normally interfaced directly, providing an attractive clamping force that can tolerate minor misalignments between the two docking surfaces. SMA devices are used mainly to drive latching mechanisms and require some type of biasing spring or other restorative element to return the SMA wire to its extended position. The main disadvantage of electromagnets and SMA devices is their power consumption, as both require consistent current to maintain the coupling force.

2.3. Symmetry

The symmetry of a coupling mechanism is dependent upon the redundant placement of interfacing features around the roll axis of the connector. When two modules approach each other, their orientations must be aligned in such a way that connecting features can properly engage. By increasing the number of coupling features, two or more docking orientations become possible, relieving roll alignment constraints during the procedure. While a coupling mechanism that is asymmetric can only dock in one specific orientation, a mechanism that is two-times axisymmetric can dock in two orientations, at offsets of 0° and 180° , and a fully axisymmetric mechanism can dock at any offset angle.

2.4. Misalignment tolerance

To increase the probability of successful coupling, modules must align opposing interfaces within an allowable range of tolerance that is dependent on the design of the connectors. Positional and rotational alignments are adjusted under the guidance of sensors and feedback control algorithms. However, exact alignment may not be possible due to sensory feedback and steady-state controller

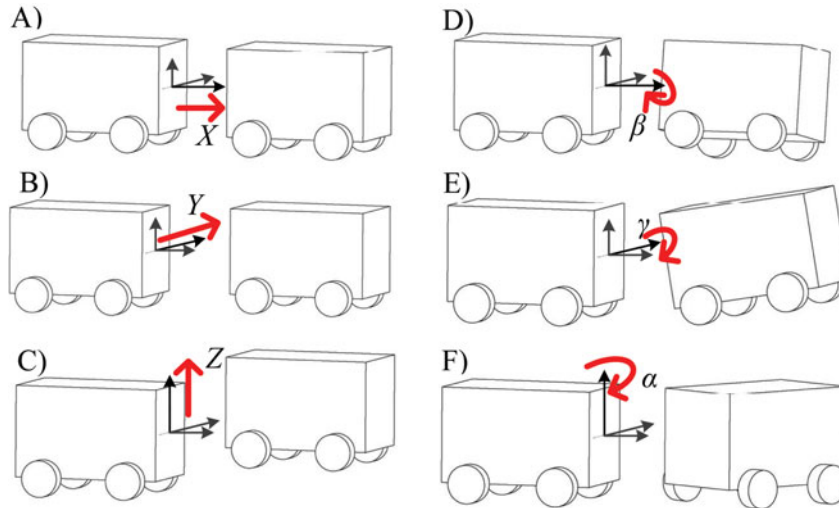


Fig. 2. Misalignment convention: (A) X, (B) Y, (C) Z, (D) Roll β , (E) Pitch γ , and (F) Yaw α .

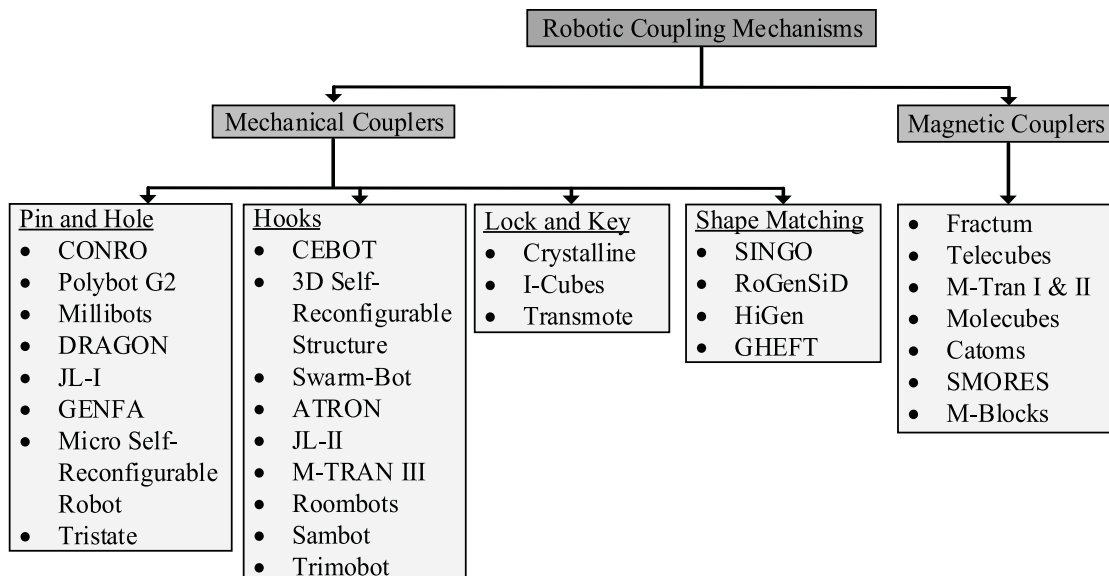


Fig. 3. Classification scheme of coupling mechanisms for modular robots.

error. Coupling interfaces must, therefore, be designed to tolerate a certain level of misalignment. To describe a mechanism’s ability to tolerate misalignments, this paper will use the convention shown in Fig. 2. The translational misalignment tolerance, Fig. 2(A)–(C), is represented as $\pm X, Y, Z$, while the rotational misalignment tolerance, Fig. 2(D)–(F), is represented as $\pm\beta, \gamma, \alpha$, where β, γ , and α represent the roll, pitch, and yaw directions, respectively.

3. Classification

The coupling mechanisms reviewed in this paper can be broadly classified into two main categories based on the types of forces acting that enable an established connection, as shown in the classification scheme in Fig. 3. The category “mechanical couplers” covers mechanisms that rely on mechanical locking between the coupling interfaces, while “magnetic couplers” utilize electromagnetic forces to establish and maintain connections. As seen in Fig. 3, the mechanical couplers can be further subcategorized into different groups based on their design principles and the type of mechanical elements incorporated into the docking interface. In the context of this classification scheme, a

comprehensive review of mechanical and magnetic coupling mechanisms will be presented in Sections 4 and 5, respectively.

4. Mechanical Couplers

4.1. Pin and hole

One of the most common designs of mechanical connectors features a set of pins and holes on the two opposing modules. After the pins are inserted into their corresponding holes, an additional mechanism locks the pins in place to prevent undesired disengagement. Among the common methods used to lock connections is the use of a mechanical latch actuated by an SMA wire. Some connectors use a combination of metal springs and SMA wires to secure the position of the pins, while still others use motorized actuators to achieve the same function.

Pin-and-hole mechanisms can generally be scaled to the size of the modules and offer a compact solution for miniature robots. They are also relatively easy to orient; once the two faces are aligned, a simple linear motion will force the pins into the holes. By using tapered pins and holes, this mechanism can also offer some tolerance for misalignment. The major drawback of this approach is the requirement of additional mechanisms for locking the connection. As mentioned above, SMA wires are commonly used for this purpose, which entails supplying an electric current through the SMA wire to raise its temperature and restore its shape. This process takes several seconds and consumes a significant amount of energy, and can therefore affect the overall efficiency and practicality of the connector. The following subsections present coupling interfaces that feature pins and holes as their primary means of docking.

4.1.1. CONRO (2002)/ PolyBot G2 (2002). The CONRO^{2,11,12} system makes use of a gendered pin-and-hole coupling mechanism, shown in Fig. 4(A.i). CONRO modules are two-degree of freedom (DOF) robots, each with a length of 21.8 cm, which are intended for reconfiguration into different mobile structures. Each module is composed of two sections that can rotate with respect to each other along two orthogonal directions. This allows an individual module to locomote and orient itself during docking, and enables a chain of the modules to perform sequential inchworm or serpentine locomotion gaits. Two modules dock by using a slithering movement to orient themselves along the same line, using intensity readings from an infrared (IR) sensor to check relative orientation. In the case of slithering, orientation and forward motion are coupled, so docking is accomplished at low speed and requires alternately checking orientation and the distance between modules. Higher speed snake docking could be accomplished by modeling this relationship and carefully synchronizing the serpentine motion of the two robots.

As shown in Fig. 4(A), the passive face of the CONRO connector has two protruding tapered pins, with grooves cut along their circumference. On the inside of the active connector, a spring-loaded propeller-shaped engagement latch partially covers the docking holes. An SMA wire is coiled around the shaft of this latch, run around rollers, and attached to a binding post. Along with the engagement latch, a disengagement latch is also embedded in the active connector and constrained to the same axis, as shown in Fig. 4(A.ii). Also included on both faces of the mechanism, but not shown in the figure, is the IR transmitter–receiver pair used to provide feedback for alignment control. During the coupling procedure, the pins of the passive face are inserted into the holes of the active face, where they push the engagement latch and cause it to rotate. Being spring loaded, the latch rotates back into the grooves of the pins, locking them in place and simultaneously pushing the disengagement latch onto them. This causes the pins to protrude through the disengagement latch, as shown in Fig. 4(A.ii). To disengage, the SMA wire is activated in order to rotate the latches in the opposite direction and release the pins. The design of the latches and the positioning of the pins make the coupling interface of the CONRO modules geometrically two-times axisymmetric, and the modules are capable of docking at a 180° offset.

A similar mechanism was adopted for the PolyBot G2 modular robot.^{13,14} This robot evolved from a previous generation, the PolyBot G1,¹⁵ which also incorporated coupling mechanisms, although these were manually operated.¹⁶ As shown in Fig. 4(B), the G2 modules have a bi-gendered connector that utilizes a pin-hole mechanism. Each connector has four tapered pins with deep grooves and four chamfered holes. On the opposing side of the connection plate, there is a spring-loaded

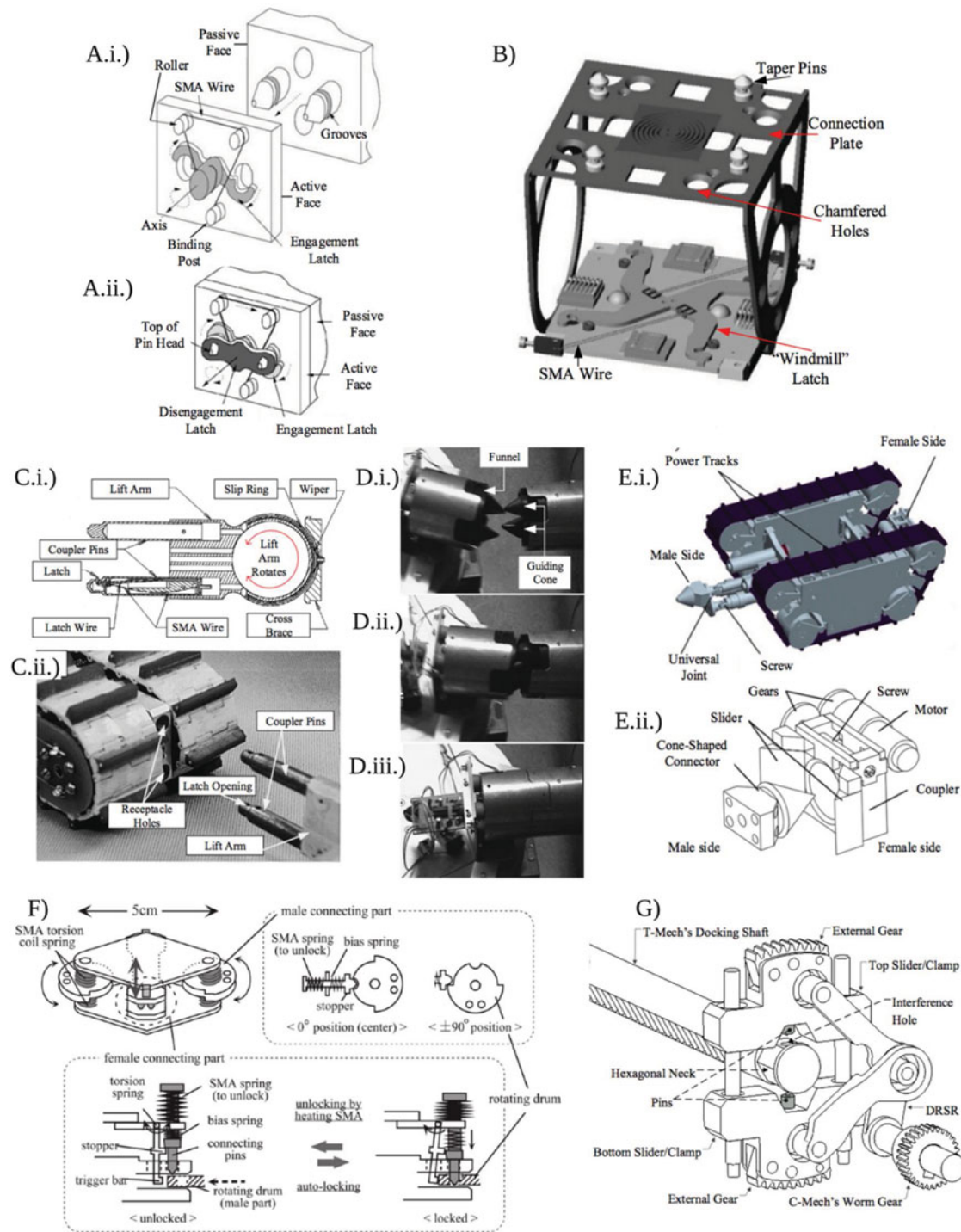


Fig. 4. Pin and hole coupling mechanisms: (A) Schematic of the CONRO coupling mechanism,^{2,11,12} illustrating: (i) Coupling procedure and (ii) Coupled configuration. (B) PolyBot G2 coupling mechanism schematic.^{13,14} (C) Millibot modular robot^{16,17} showing: (i) Schematic diagram of male coupling interface and (ii) Concept of coupling between two modules. (D) DRAGON connector^{9,18} coupling procedure: (i) Modules approach each other, (ii) Conical features self-align, and (iii) Connectors latch together. (E) JL-I coupling mechanism, showing: (i) CAD rendering of JL-I robot module and (ii) Schematic view of the coupling mechanism.^{19–21} (F) Schematic diagram of the Micro Self-Reconfigurable Robot coupling mechanism.^{24,25} (G) Schematic diagram of the Tristate coupling mechanism.^{26–28}

windmill-shaped latching device that serves the same function as the engagement latch on the CONRO modules. As the pins are inserted into the holes, they cause the latch to rotate, thereby compressing its springs. With the pins fully inserted, the springs push the latch back in the opposite direction to lock the connection and hold the pins in place. Once engaged, the two modules can share power and data using electrical connectors embedded in the connection plate. Like the CONRO modules, the PolyBot G2 modules use IR sensors to align the two opposing connectors. As each PolyBot module possesses only a single (rotational) DOF, the system's capacity to properly align and orient itself during docking is less than that of CONRO. The approach of PolyBot is to offset its fewer DOFs by an increase in the axisymmetry of the coupling interface. While the connectors used in the CONRO modules are two-times axisymmetric, the PolyBot coupling interface is four-times axisymmetric and can be connected at an offset of 0° , 90° , 180° , and 270° . This setup reduces the complexity of the alignment process and enhances the efficiency and flexibility of the modular robot.

4.1.2. Millibots (2002). The Millibots robotic platform^{17,18} is a $4.1 \text{ cm} \times 6.4 \text{ cm} \times 10.9 \text{ cm}$ tread-driven robot intended for forming train-like structures to traverse difficult terrain. Figure 4(C.i) shows the male side of the coupling mechanism, which features two tapered coupling pins attached to a lift arm with a rotating slip ring mechanism. The lift arm is used to align the connectors during the coupling procedure and is also used to lift neighboring modules to traverse uneven terrain. Inside the lower pin is a latch made from a combination of piano wire and SMA wire. The SMA wire is electrically connected back to the main body of the robot via the slip ring, thus minimizing the risk of cable fatigue or interference. The female side of the mechanism, Fig. 4(C.ii), has two receptacle holes and an internal feature where the latch of the male pin engages and locks the connection. To decouple, the SMA wire is activated to retract the latch, allowing the robot to disengage. After disengagement, the latch returns to its original position under the elastic force of the piano wire. The Millibots coupling system is asymmetric and docking can only occur in one orientation. Furthermore, the system is not failsafe, as disengagement can only be initiated by the male side. Millibot's success in employing an asymmetric docking configuration owes to the high amount of maneuverability imparted by its two sets of two tracked wheels, which, assuming use on a flat plane, provide greater mobility than the crawling-type gaits employed by other modular robots.

4.1.3. DRAGON (2002). The DRAGON^{9,19} connector, shown in Fig. 4(D), is a bi-gendered coupling mechanism with a diameter of 75 mm. It consists of two guiding cones, two funnels, a rigid sheath, and a band of spring steel embedded along the inner circumference of the sheath. The inner side of the spring steel has a piece of SMA wire attached to it. Although the DRAGON connector does not have pins and holes, its function is similar to the other connectors in this category; the cones act as the pins by aligning the connectors together as they are pushed into the funnels, and the spring band acts as the additional mechanism used to lock the connection. As shown in Fig. 4(D.i–D.iii), the outer shells of the two connectors lock together, thereby forcing the spring band of each connector into a channel on the interior surface of the opposing connector. The springs then push against the inner wall of the shells, holding them together and preventing any accidental disconnection. To undock, the SMA wire is activated, which shrinks and compresses the springs inward, releasing the connectors. Despite being only 0.5 mm thick, the spring bands can hold a load of up to 700 N and a bending torque of 117 N·m. The authors have demonstrated the connector's reliability by suspending a human from an elevated height. The coupling interface uses IR transmitters in the cones and corresponding receivers in the funnels as beacons during the docking process. Once the connection is successful, they are also used to transfer data between the two connected modules, along with 12 electrical contacts used for power transfer. The DRAGON connector is two-times axisymmetric and can mate at offsets of 0° , 90° , and 270° .

4.1.4. JL-I (2006). The JL-I robotic platform^{20–22} represents a macro-size implementation of modular robots that are designed to navigate on rough terrain. Each module, as shown in Fig. 4(E.i), is composed of two tracked units with dimensions $35 \text{ cm} \times 15 \text{ cm} \times 25 \text{ cm}$ that make use of a gendered coupling mechanism to connect to neighboring modules in a snake-like formation. Fig. 4(E.ii) shows the coupling mechanism employed by the JL-1 modules. The cone-shaped male connector has a deep notch on its wide end and tapers to a point, while the female surface features a conical cavity and two sliders actuated by a power screw. The inner surfaces of the sliders are angled so that they passively guide the male cone into the cavity, compensating for misalignment. During the coupling procedure,

a 3-DOF universal joint is used to align the cone with the female receptacle. After the male connector is inserted into the cavity, the sliders move inward along the back side of the cone and lock it in place. With the two modules connected, the same 3-DOF joint can be used to lift and rotate the adjacent module. With the 3-DOF mechanism used for alignment and with the sliders acting as passive guides, the JL-I module achieves high misalignment tolerance up to $\pm 30, 30, 30$ mm and $\pm 45, 45, 45^\circ$. However, the established connection is not failsafe, as the female side must be operational to disengage.

4.1.5. GENFA (2011). The GENderless and FAilsafe (GENFA) connector²³ is designed for the REPLICATOR robotic platform²⁴ and has face dimensions of 50 mm \times 40 mm. GENFA incorporates two sets of pins and holes mounted on two disks. The outer disk features four mushroom pins and can be rotated using a gear motor, while the inner disk is stationary and has four tapered pins and holes. By inserting the pins into their corresponding grooves, two translational DOFs and three rotational DOFs are constrained. To constrain the last DOF and prevent any movement normal to the coupling surface, the outer ring rotates, locking the mushroom pins in the narrow end of the opposing cutout channel.

Unlike the coupling mechanisms discussed in this category so far, GENFA uses a motorized mechanism to lock the connection instead of SMA wires. This mechanism consists of a gear motor and a worm gear assembly, used to actuate the rotary disk as explained above. As opposed to SMA wires, this mechanism offers a more energy-efficient, non-back drivable solution; the motor only needs to be briefly powered during the coupling procedure, since the worm gear prevents any rotation in the opposite direction once the pins are engaged. Furthermore, the GENFA mechanism is failsafe, as the connection can be broken from either side. Because the system is four-times axisymmetric, coupling can be achieved at an offset of 0° , 90° , 180° , and 270° .

4.1.6. Micro Self-Reconfigurable Robot (2013). The Micro Self-Reconfigurable Robot^{25,26} is designed for small-scale applications and has a cubic profile measuring 3 cm³. As seen in Fig. 4(F), the male side of its coupling mechanism consists of a rotating drum that is roughly circular in shape, with two holes to accommodate the female pins. The drum, which is actuated by two SMA springs, can rotate 90° in either direction and is locked in place at the end of this range of motion by a stopper. The female pins use bias springs and a stopper to lock, and an SMA spring to unlock. During coupling, the male drum is inserted into the female receptacle, pushing back the trigger bar that moves the stopper and releasing the spring-loaded pins into the holes. The connectors are asymmetric, and can only couple with each other in one orientation. While connected, embedded electrodes enable the transmission of data across modules. To disengage, the SMA springs are heated, drawing the pins back up and allowing the removal of the male drum. This mechanism is not failsafe, as the female side must be active to disengage. Critical to designs of this type are the response time and torque generated by the SMA actuators. Motion of individual modules is in this case supplemented by complementary rotation and releasing of coupling components by adjacent modules.

4.1.7. Tristate (2014). The Tristate^{27–29} is a gendered, non-back drivable coupling mechanism designed for the modular robot STORM.^{30,31} It consists of a male connector, referred to as C-Mech, and a female connector, referred to as T-Mech. As shown in Fig. 4(G), the T-Mech consists of a docking shaft with a hexagonal neck that can be extended outward from either side of the module. The C-Mech features a Dual-Rod Slider-Rocker mechanism (DRSR), which switches between three modes of operation: the drive mode, the neutral mode, and the clamp mode. The clamps are designed with external gears on the outside. In the drive mode, the external gears of the clamps engage with the inner gears of the coupler, as shown in Fig. 4(G), and the torque supplied by the central motor is used to drive the tracks of the module. In the clamp mode, the clamps are driven inward to engage the pin with the holes on the T-Mech. In this mode, the torque supplied by the central motor is used to rotate the connected module with respect to its neighbor, while no energy is required to maintain the connection since the clamps are driven by a non-back drivable worm gear transmission. The neutral mode is used to align the clamps to the docking shaft by disengaging them from both sides and rotating them freely.

Incorporating torque circulation through the DRSR allows the C-Mech to be actuated through the central motor of the STORM module in all three modes. This eliminates the need for actuating the docking interface separately and, along with the compact design of the DRSR mechanism, gives

the C-Mech coupler a small footprint, only 77 mm in width. The Tristate mechanism is six-times axisymmetric, owing to the hexagonal arrangement of pinholes on the docking shaft.

4.2. Hooks

Another family of coupling mechanisms incorporates hooks or grippers on one side of the connection and holes, grooves, or rods on the opposing side. Grippers can typically be retracted into a module or folded onto its surface, thus occupying little or no external space in the disengaged state. More importantly, coupling and disengaging the hooks with their receptacles requires only a single motion, without the need for additional mechanisms or latches to lock the connection. This approach offers a simpler, faster, more compact solution in the design of reconfigurable robots consisting of a large number of modules. A gripper may also possess some additional manipulation capabilities and is potentially useful in unstructured environments, since it can be more flexibly oriented in space. However, a gripper can be more challenging to control, since its end effector must be correctly positioned for a connection to be successful. Coupling mechanisms employing hooks or grippers are presented in the following subsections.

4.2.1. CEBOT (1988). Developed in 1988, the Cellular Robotic System (CEBOT)^{32–34} is considered one of the first robotic platforms to be introduced in the field of modular robotics. The coupling mechanism used in a CEBOT module, shown in Fig. 5(A), has a gendered, asymmetric design that consists of two latching hooks on the male side, and two latching posts on the female side. The male side of the mechanism is housed within a cone-shaped protrusion, which mates with a similarly shaped indentation on the female side. The latching hooks are actuated by a non-back drivable worm gear assembly driven by a DC motor. Using sensory feedback from photodiodes built into the coupling interface, the male connector is driven into its receptacle. The hooks are then rotated to grasp the latching posts, thereby locking the connection. Once coupled, 14 pin connectors establish communication and power transfer between the modules. To disengage, the hooks are rotated in the opposite direction and the male cone is removed.

4.2.2. 3-D Self-Reconfigurable Structure (1998). The 3-D Self-Reconfigurable Structure, proposed by Murata *et al.*,^{35,36} uses a bi-gendered coupling mechanism with spring-loaded hooks. As seen in Fig. 5(B), each side of the coupling mechanism has two hooks and a central connecting head with a concave channel that interfaces with the hooks. The hooks are moved using a connecting cuff that slides along the head, rotating them inward to clamp down on the central head of the opposing connector. Once coupled, the connecting hands transmit non-back drivable rotational torque to the other module via a worm gear mechanism. A DC motor with a harmonic drive actuates both the power screw of the connecting cuff and the rotating arm. To switch between these two modes, an electromagnetic clutch is used to engage the power screw and start the coupling procedure. This mechanism is two-times axisymmetric, and the opposing connectors must be at an offset of 0°, 90° or 270° to dock.

4.2.3. Swarm-Bot (2005). The Swarm-Bot^{37,38} is a cylindrical, wheeled robotic module, featuring an extensible claw-shaped gripper-arm and a coupling ring that spans its circumference. The robot uses two sets of tracks and two wheels located externally (radially) with respect to the tracks, which provides high stability and efficient zero-radius of curvature rotation. As seen in Fig. 5(C.i), the geometries of the claw and the ring are designed to match each other while offering some tolerance for misalignment. Each claw has an embedded light sensor and LEDs, shown in Fig. 5(C.ii), which are used to determine if an object is present for gripping and to confirm a successful grip. The light sensor is also used to detect the LEDs of the coupling ring. These LEDs light in different colors to indicate whether the module is available for docking or not. Coupling is achieved when the claw detects the coupling ring and grasps it with a force of 15 N. The claw-arm linkage is able to telescopically extend and contract, so that the connection between modules is flexible and variable in length. This feature allows robot chains to actively change shape and exert forces on each other while linked. The high-maneuverability of the claw-arm and the full axisymmetry of the coupling ring also potentially allow for a large number of robots to simultaneously dock to the same module.

4.2.4. ATRON (2006). The ATRON module^{39,40} is composed of two roughly spherical hemispheres, 11 cm in diameter, which can be rotated with respect to each other around their central axis. Each hemisphere has two female connectors and two active male connectors. The male connector consists of three claws, as shown in Fig. 5(D). The two outer claws rotate axially outward, while the inner

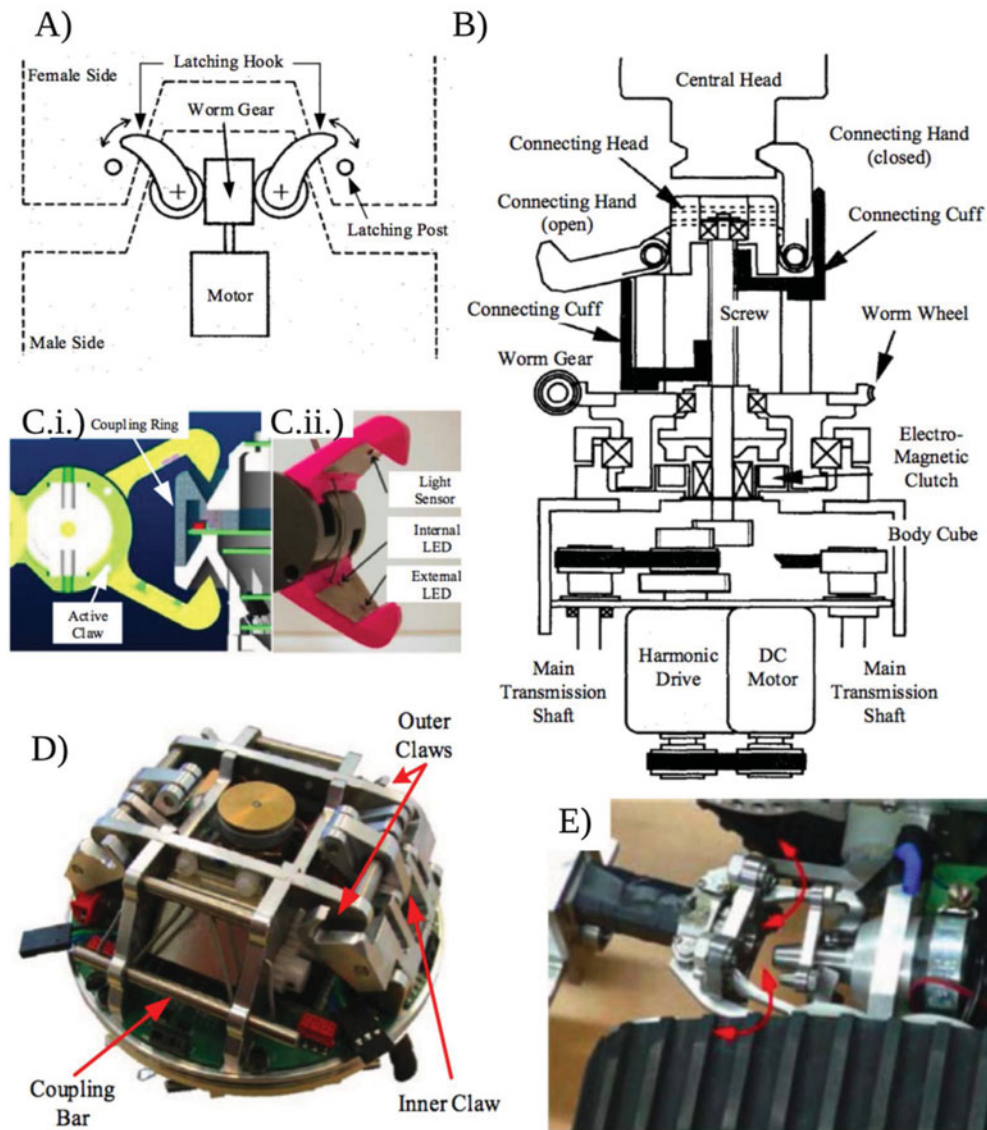


Fig. 5. Hook Coupling Mechanisms: (A) Schematic of CEBOT coupling mechanism.^{31–33} (B) Schematic diagram of the 3-D Self-Reconfigurable Structure.^{34,35} (C) Swarm-Bot^{36,37} coupling procedure: (i) Schematic view of active claw and coupling ring during gripper approach and (ii) Photograph of the coupling claw with indicated sensors. (D) Photograph of an ATRON module without its plastic protective cover.^{38,39} (E) The JL-II coupling mechanism⁴⁰ depicting the claw locking onto the cone during the grasping phase.

claw rotates inwards, toward the module. The female side has three rigid coupling bars for interfacing with the claws. In the uncoupled state, the claws can be completely retracted within the body of the module. This coupling method is asymmetric, and the coupling bars have to be parallel to the axis of the claws for a successful connection. To couple, a lead screw driven by a DC motor pushes the claw linkage outwards, latching the claws onto the coupling bars. Although this coupling mechanism requires accurate orientation, the established connection is roughly one-dimensional. This, along with the module's spherical design, allows for a wider range of rotational movement between the connected modules. As each module is fully circular along its central axis, it can be used as a wheel, enabling a variety of interesting locomotion modes, including an “intelligent conveyor surface” and a variety of modular car configurations. The location of the coupling mechanisms on the surface of the hemispheres is, therefore, an important consideration in this design to prevent impeding 360° rotation in the modules that are employed as wheels. Each ATRON has only a single DOF, the relative rotation of its two hemispheres, and has limited mobility on its own. To overcome this limitation,

when ATRON modules decouple from the full lattice structure, they do so in a group of three, termed a “meta-module.” (Note that any individual module is allowed to move between meta-modules.)

4.2.5. JL-II (2010). A second generation of the JL-I platform, called the JL-II,⁴¹ was developed and introduced in 2010 with a modified coupling mechanism. Instead of the cone-shaped protrusion on the male side, a gripper was incorporated in the new design. In addition to functioning as a coupling mechanism, the gripper in the JL-II robot can also be used for manipulation. As seen in Fig. 5(E), the gripper is opened and closed using a power screw that pushes against the base of the claw, moving the fingers with a cam slot mechanism. The claws of the gripper are semi-circular and form an elliptical hole when brought together. During the coupling procedure, the gripper is brought into proximity with the cone-shaped female connector. After the gripper grasps around the back side of the female connector, its base is extended outward until it engages with the main docking cone and the four sub-docking cones found on the female surface. The male connector is not symmetric, but the female connector is four-times axisymmetric and can rotate according to the orientation of the gripper. As in JL-I, the JL-II connector is not failsafe, as the male side must be functional in order to disengage. The coupling mechanism used in the JL-II modules has a significantly lower tolerance for misalignment than its predecessor, owing to constraints on the orientation of the gripper, and can thus only tolerate translational misalignment of $\pm 2, 5, 5$ mm and rotational misalignment of $\pm 10, 10, 10^\circ$. However, the robust spherical joints formed at the coupling points combined with the use of tracked units allows a chain of the robots to make large posture changes and can provide enough torque to completely lift a module off the ground.

4.2.6. M-TRAN III (2008). M-TRAN III⁴² followed two generations of the M-TRAN modular robots introduced in 2002 and 2003. The coupling mechanism incorporated into M-TRAN I and II uses permanent magnets, and will be discussed in Section 5.3. The M-TRAN III module is 65×65 mm \times 30 mm in size and, aside from its coupling mechanism, is mostly unchanged from previous versions. Each module is composed of two subsections that rotate with respect to each other along two parallel rotational-DOFs, which when combined with the subsections’ rounded-cylinder shape, enable an inchworm-like gait. This setup also allows for reliable placement of the modules in a lattice structure, using a series of 90° and 180° rotational maneuvers. As seen in Fig. 6(A), the active face of the coupling mechanism used in M-TRAN III has four hooks offset at 90° intervals, each connected to a sliding block. The hooks lie flush with the active face of the mechanism in the disengaged state. During the coupling procedure, the sliding blocks are pushed outward by a non-back drivable gear motor, causing the hooks to rotate and extend out of the plate. The hooks then latch into the triangular grooves found on the female side. As shown in Fig. 6(A), the face of the connectors also features a set of electrodes used to share data between the connected modules. Due to the shape of the hooks and grooves, the M-TRAN III connector can tolerate up to $\pm 2, 5, 5$ mm translational and $\pm 10, 10, 10^\circ$ rotational misalignment. In 2006, a module with an additional camera was investigated to improve coupling on flat terrain using visual feedback.⁴³

4.2.7. Roombots (2010). The coupling mechanism of the Roombots^{44–46} modular robot, shown in Fig. 6(B.i), is similar to that of M-TRAN III. Roombots “meta-modules” consist of two hemispherical pairs with a diameter of about 45 mm, each featuring a bi-gendered coupling mechanism, and are intended for reconfiguration into furniture and home fixtures. Each pair of hemispheres can rotate with respect to each other, and a third DOF is supplied by the swiveling joint between the two spheres. A variety of locomotion modes and reconfiguration strategies is open to the system as a result of its high number of DOFs, including an inchworm like mode during reconfiguration. Each connector has four hooks and four latching ports. The latching ports are offset from the hooks by a little less than 90° , as seen in Fig. 6(B.ii). The connector is four-times axisymmetric and is not failsafe as both sides must be powered to undock. With the connectors engaged, the central motor of the module can transmit up to 7 N·m of rotational torque. Undocking experiments demonstrated that decoupling under strain was less successful than in strain-free states. The creators of the Roombots envisioned that the robots could be used jointly with passive building blocks equipped with similar coupling interfaces. In these cases, the tasks of detection, alignment, and establishing connections would be the sole responsibilities of the active modules, and might, therefore, require them to carry extra actuation and sensing equipment. Disengagement would also depend completely on the active module, and would, therefore, not be failsafe.

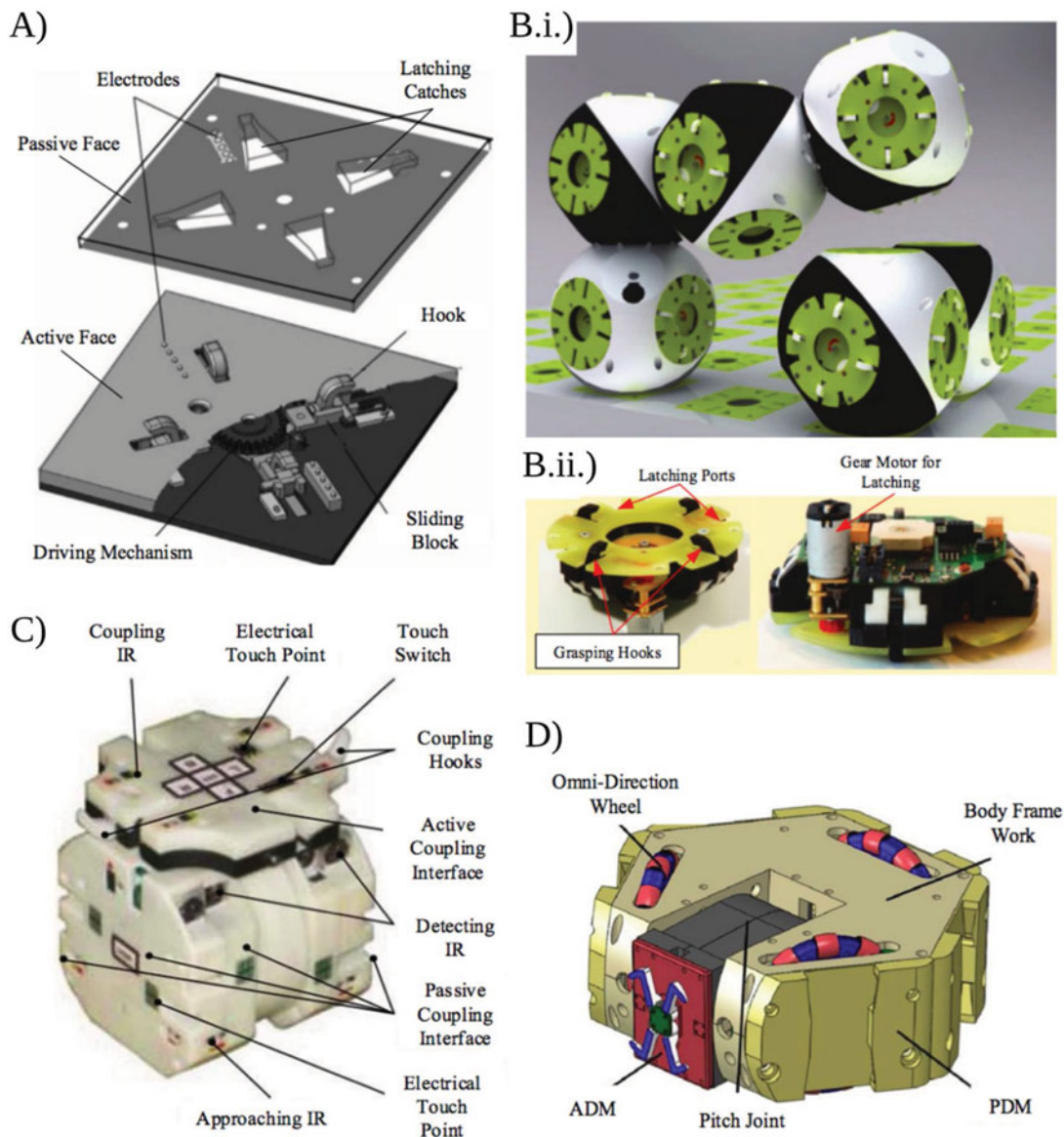


Fig. 6. Hook Coupling Mechanisms (contd.): (A) Schematic of the M-TRAN III coupling mechanism.⁴¹ (B) Roombot coupling mechanism, showing: (i) Rendered visualization of connected Roombots modules and (ii) The active connection mechanism.^{43–45} (C) Sambot module.^{46–48} (D) CAD renderings of the Trimobot platform and coupling mechanism.⁴⁹

4.2.8. *Sambot* (2011). The Sambot module^{47–49} has dimensions 80 mm × 80 mm × 20 mm and features one active and four passive coupling interfaces. As seen in Fig. 6(C), the active interface has two coupling hooks protruding from the sides, while the passive interface has coupling grooves. This coupling mechanism is two-times axisymmetric, and the connectors can be coupled at offsets of 0° and 180°. Each Sambot module is equipped with two wheels on its bottom surface, allowing for navigation and orientation changes via differential drive. Using IR sensors, the modules are brought into close proximity, and once the active interface makes contact with the passive, electrical touch points connect and the coupling procedure begins. The hooks are then turned by a gear motor until they engage with the grooves of the opposing module. The same electrical contacts that initiate the connection are used for communication and power transfer between the modules. The Sambot coupling mechanism can tolerate up to ±13, 4.5, 19.5 mm translational and ±5, 5, 10° rotational misalignment.

4.2.9. *Trimobot (2016)*. The Trimobot⁵⁰ robotic platform, shown in Fig. 6(D), uses a gendered coupling mechanism with two connectors, an “Active Docking Mechanism” (ADM), and a “Passive Docking Mechanism” (PDM). The face of the ADM is 27 mm × 43 mm and consists of four hooks attached to spur gears. One of the four hooks is mounted on a stepper motor and drives the rest of the hooks through the gears attached at their bases. The PDM has four channels that interface with the ADM hooks. Three omnidirectional wheels allow the modules to locomote and control their orientation. To couple, an ADM of one module is brought into the channel of the PDM. The stepper motor then rotates the hooks, locking the connection between the two modules. Decoupling is accomplished by reversing the rotation of the motor. This connection mechanism is two-times axisymmetric and is not failsafe, as the male connector must be active to undock. A camera is also added to the ADM to aid the coupling procedure.

4.3. Lock and key

The coupling mechanisms in this category operate in a similar way to the pin-and-hole mechanisms. Instead of the pins, these connectors feature especially designed keys that are inserted into a cavity on the female surface. The key is then rotated through channels embedded within the cavity, locking the connection. Actuating this type of mechanism typically requires only one motion. However, the unique shape of the key should be designed to tolerate misalignments between modules, which could potentially complicate the self-reconfiguration procedure. Notable examples of lock-and-key coupling mechanisms are discussed below.

4.3.1. *Crystalline (2000)*. Crystalline^{51,52} is a planar, lattice-type modular robotic system that uses the gendered lock-and-key connector shown in Fig. 7(A). Each “Atom” module stands two inches tall and contains a central rack-and-pinion mechanism that extends its four sides linearly outwards. The module occupies two square inches when contracted and four when expanded. Two of the module’s faces carry an active connector, consisting of a bar-shaped key mounted on a DC gear motor. The remaining two faces carry the passive channel illustrated in the figure, which is designed to have internal cavities, or pockets, to accommodate the key. During the coupling procedure, the key is first inserted into the channel and then rotated 90° about its central axis to lock the connection between the two faces. Because the Crystalline connector has active and passive sides, it is not failsafe. However, it provides a simple, compact coupling mechanism.

Individual Atoms can employ contraction and expansion phases to perform inchworm locomotion. Linking many modules together in a lattice structure, the shape-changes of individual modules can be used to move the entire robot “crystal” or alter its shape. Coupling with a module already bound in a lattice is simplified by the increased stability provided by the additional modules, whereas two unbound modules would have to carefully synchronize inchworm motion with the coupling procedure. Atoms modules or meta-modules can be repositioned on a lattice using an “inchworm propagation algorithm.” Because of the compressibility of the modules, they can also move through the volume of a lattice, by a process in which a unit is pushed along by the contractions and expansions of its neighbors. This complex behavior is enabled by the fact that each inter-Atomic interface contains one active and one inactive connection mechanism, though for the same reason, independent orientation changes of individual modules are not possible.

4.3.2. *I-Cubes (2001)*. In principle, the coupling mechanism developed for the I-Cubes^{53,54} robotic system, shown in Fig. 7(B), operates in the same way as the Crystalline connector. An I-Cube module is 8 cm³ in volume and carries female connectors on each side and a cross-shaped key on one side. The key is 16 cm in length and has one rotary-DOF. To connect two modules, the key is first inserted into the cavity on the opposing female connector. Embedded within the cavity are two latching pegs actuated by a servomotor, as indicated in Fig. 7(B). These are retracted into the body of the module to allow the key to rotate into the locked position. The latches are then released to prevent any rotation of the key in the opposite direction. Misalignment tolerance of the I-Cubes mechanism is not provided in detail, but the chamfered edges of the cross-shaped cutout are intended to allow for tolerance of minor misalignments.

4.3.3. *Transmote (2012)*. The connector used in the Transmote⁵⁵ robotic platform, pictured in Fig. 7(C), is another example of a gendered lock-and-key coupling mechanism designed with the intent of autonomous home network security system repair.⁵⁶ With reference to Fig. 7(C.i), the male

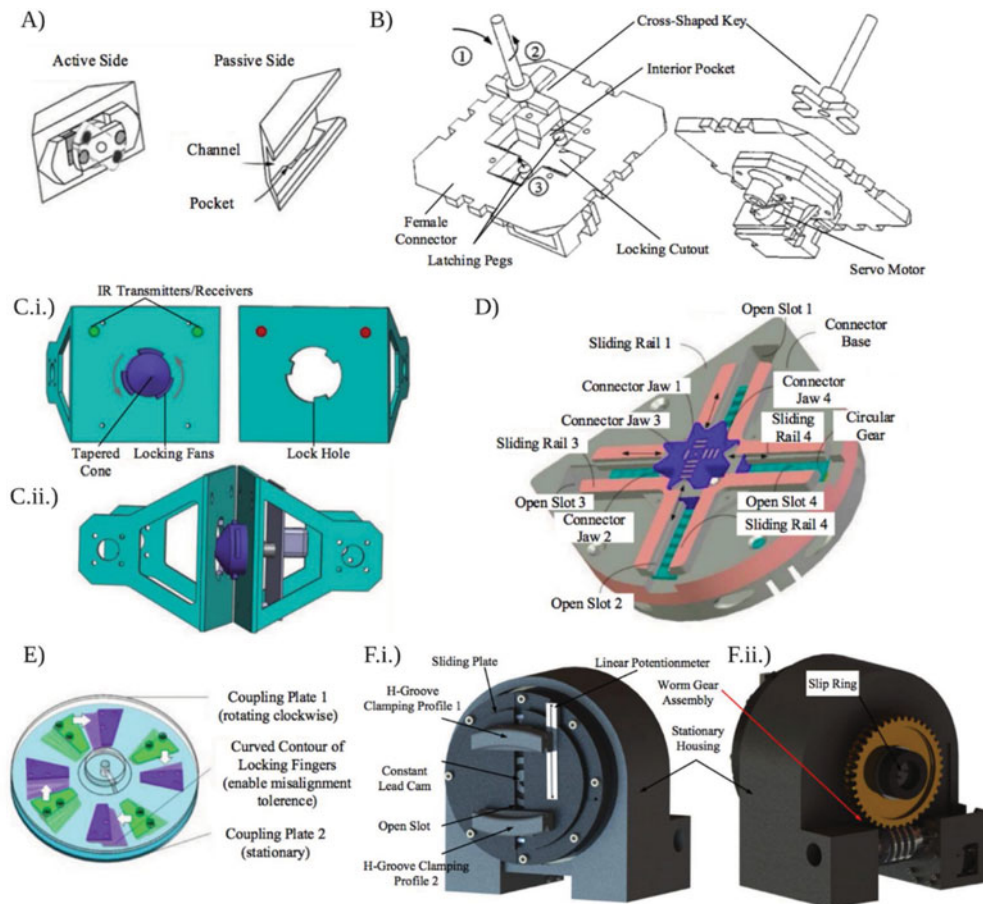


Fig. 7. Lock and key coupling mechanisms: (A) Coupling mechanism for the Crystalline modular robot.^{50,51} (B) Schematic showing the docking process for I-Cubes.^{52,53} Numbers illustrate the coupling procedure: (1) Insertion, (2) Rotation into grooves, and (3) Latching pegs extended. (C) CAD rendering of the coupling mechanism on the Transmote modular robot:⁵⁴ (i) Male and female coupling interfaces and (ii) Alignment procedure. (D) SINGO coupling mechanism.⁵⁶ (E) Schematic of RoGenSiD coupling mechanism. Here, the mechanism is shown unlocked, with the plate rotating toward the locked position.⁶⁰ (F) CAD rendering of the GHEFT coupling mechanism,^{63,64} illustrating: (i) Front view and (ii) Rear view.

side of the connection has a tapered cone with three fan-shaped locking plates and the female side has a lock hole with the same profile. The cone is affixed to a shaft that is connected to a servo motor. Both the male and female surfaces are equipped with IR transmitters and receivers, which are used to communicate the relative location and orientation of the modules during the alignment process shown in Fig. 7(C.ii). As opposed to the I-Cube modules, docking the Transmote modules only requires inserting the key into the female surface and rotating it, without the need for an additional mechanism to lock the connection. The Transmote coupling mechanism can tolerate up to $\pm 0, 30, 30$ mm translational and $\pm N/A, 15, 15^\circ$ rotational misalignment. In the roll direction, the male cone can be actively adjusted to compensate for misalignment.

4.4. Shape matching

The category of shape matching coupling mechanisms encompasses identically shaped connectors that rely on their geometry to establish a connection between them. The profiles of these connectors feature especially designed geometries that allow them to interlock and engage together, preventing any relative motion. This design principle is particularly suitable for genderless coupling interfaces, as both connectors are identical. The mechanisms typically provide a failsafe connection, as the connection can be broken from either side. However, this is not always the case; depending on their design and their actuation, such connectors might require additional mechanisms to constrain any

remaining DOFs or prevent undesired disengagement. The following subsections present the coupling mechanisms using this approach.

4.4.1. SINGO (2009). SINGO⁵⁷ is a genderless coupling mechanism designed for implementation on the SuperBot platform.^{58–60} As seen in Fig. 7(D), the SINGO mechanism uses four chevron-shaped “jaws” that can move radially along linear sliding rails on the surface of the connector. The connector is 64 mm in diameter, and the jaws can open from 15 mm to 50 mm apart. The four jaws have an angular undercut that prevents movement normal to the face of the connector and are actuated by a single circular gear with a helical groove machined on the top surface. As the gear spins, it pushes the jaws out or draws them back toward the center of the connector. During the coupling procedure, the jaws on the two opposing connectors are moved in opposite directions until they meet and engage. The central gear is actuated by a micro-DC motor and is non-back drivable, eliminating the need for any power consumption once a connection is established. Disengagement requires moving the jaws in the opposite direction and can be achieved by either side of the connection, which makes the mechanism failsafe. The angled geometry of the SINGO jaws allows for a tolerance of $\pm 6, 5, 5$ mm translational and $\pm 6-22, 5, 5^\circ$ rotational misalignment, depending on the position of the jaws.

4.4.2. RoGenSiD (2013)/HiGen (2016). The Rotary Genderless Single-sided Coupling mechanism (RoGenSiD),⁶¹ pictured in Fig. 7(E), was developed for the ModRED modular robot.⁶² RoGenSiD is a single-sided failsafe coupling mechanism with an interface that consists of a rotating coupling plate with four steel latching fingers attached to it in a circular array. The Z-shaped fingers are designed with a lower protrusion and an overhang feature that allow two identical fingers to engage together from either side. To lock the roll-DOF, a set of tapered alignment pins and holes are used to prevent the modules from rotating around their axes and to ensure that the fingers remain in place.

The coupling procedure consists of two steps. First, the two modules are brought near each other and the alignment pins are inserted into the holes. One plate rotates clockwise while the other remains stationary, locking the fingers together. This rotation is actuated by a geared bipolar stepper motor with a non-back drivable worm gear assembly. The RoGenSiD coupling interface also features spring loaded electrodes embedded in the alignment pins that provide power and data sharing between the modules. The tapered features on the pins and fingers can mitigate up to $\pm 20, 2, 2$ mm of translational misalignment and $\pm 2.4, 2.4, 2.4^\circ$ of angular misalignment.

A similar mechanism is used in the High-Speed Genderless (HiGen)⁶³ coupling interface. Like RoGenSiD, HiGen features latching fingers placed on a rotary disk. These fingers can also translate in the direction normal to the face of the connector. The faceplate of the HiGen connector is 71 mm in diameter and has internal helical guides. As the faceplate rotates, the fingers are drawn outward in a screw-like motion. The latching fingers have a simple L-shaped overhang design that enables them to engage with each other. The HiGen connector also features a shroud that is extended outward with the latching fingers. The shroud fulfills the same function as the pins on RoGenSiD; it locks the connection and prevents the two connectors from rolling around their axes. The shrouds also protect the fingers in the docked state. As in RoGenSiD, the HiGen connector is four-times axisymmetric. Moreover, HiGen is also single-sided failsafe, allowing for disconnection with actuation from just one module.

A geared DC motor mounted directly on the axis of the connector drives the HiGen mechanism, and the friction within the motor’s gearbox prevents back-driving. The motor is connected to an especially designed drive shaft that rotates the fingers and pushes out the shroud simultaneously. The HiGen connector also features a PCB ring with 24 electrical connection pads, which allow for power and data transmission in any of the four docking configurations. With tapered profiles in the design of the shrouds and the fingers, HiGen can tolerate translational misalignment of $\pm 13.5, 2.5, 2.5$ mm and rotational misalignment of $\pm 8, 8, 10^\circ$.

4.4.3. GHEFT (2017). The Genderless, High strength, Efficient, Failsafe, and high misalignment Tolerant (GHEFT)^{64,65} coupling mechanism uses especially designed clamping profiles to couple with identical units. The mechanism is composed of the three main subsystems shown in Fig. 7(F.i): a stationary housing, a rotating plate, and two genderless elliptical clamps with an H-shaped cross-section. The mechanism has two DOFs: (1) relative rotation between the rotating plate and stationary housing, and (2) simultaneous translation of the clamping profiles relative to the rotating plate in a fixed slot. A worm gear assembly on the rear of the GHEFT, Fig. 7(F.ii), provides rotational torque for

the rotating plate, and an internal servomotor interfaced with a constant lead cam provides translation of the clamping profiles. Both forms of actuation are non-back drivable, making the mechanism energy efficient since power is not required to maintain a connection.

During the coupling procedure, two coupling mechanisms are brought into close proximity, and the clamping profiles are actuated. The *H*-shaped clamps act as followers as the lead cam is rotated. Rotating the cam results in the clamps either moving inward or outward, resulting in a clamping force of 220 N. The clamping profiles are designed with concave surfaces that are capable of tolerating ± 6 , 28, 11 mm translational and ± 45 , 13, 11° rotational misalignment and that also provide a fail-safe connection in case a module malfunctions. An optimization procedure was presented to compute clamping profile geometry to tolerate arbitrary misalignment tolerances defined by the user. In a coupled configuration, a GHEFT mechanism can provide infinite relative rotation of modules due to an incorporated slip ring, Fig. 7(F.ii), and provide a rotational torque of up to 13 N·m.

5. Magnetic Couplers

This section reviews the coupling mechanisms that rely on magnetic forces as their primary docking method. This design approach offers several advantages when compared to some of the alternatives discussed in previous sections. Whether permanent magnets or electromagnets are used, adopting magnetic coupling generally saves space in the design of connectors by eliminating the need for actuators and other mechanical elements. This advantage makes magnetic docking methods particularly helpful in micro-scale applications. Moreover, magnets are inherently self-aligning, which simplifies the docking process and aids in fine alignment. Some notable magnetic couplers implemented in previous modular robots are discussed in the following sections.

5.1. *Fractum* (1994)

The *Fractum* robotic modules^{66,67} are approximately 125 mm in diameter and can reconfigure their structure by rotating with respect to each other in a planar workspace. Figure 8(A) shows the design of a *Fractum* module, which consists of three triangular layers that are overlaid in an offset pattern. The female side of the coupling mechanism consists of two circular permanent magnets located on the top and bottom layers of the robot. The male side of the mechanism is a circular electromagnet located in the middle layer of the robot. Optical transmitters and receivers are embedded on both sides of the connection for data transfer and communication. During the coupling process, the electromagnet embedded in the male side of the unit is activated, and is then pulled into the gap between the two outer layers. To disconnect, the polarity of the electromagnet is reversed and the resulting repulsive forces break the connection. The 2-D grid formed by the *Fractum* modules can be reconfigured by moving a module with respect to its neighbors. This is achieved by switching the polarity of the module's arms, disconnecting one arm, and connecting the other, while using the third arm as a pivot for this rotational motion. In this way, the electromagnets of the *Fractum* module serve both as a coupling interface and as a movement mechanism.

5.2. *Telecubes* (2002)

The *Telecubes* robotic platform^{68,69} is a lattice-style modular robot consisting of cubic units that occupy a footprint of 6 cm³. Each module can contract and expand normal to its faces using lead-screw linear actuators. Figure 8(B) shows the bi-gendered *Telecubes* coupling mechanism, which is composed of a square plate with four square regions on its corners. Two of these regions contain a switching permanent magnet device, and the remaining two are ferromagnetic metal plates. The switching devices consist of a spring-loaded sliding card carrying permanent magnets and actuated by an SMA wire. The sliding card shifts under a rack of other permanent magnets. In the relaxed position, the magnets on the sliding card are positioned such that the magnetic flux is routed outward and the device can attract the metal plates of another connector. In the actuated position, the sliding card is pulled so that the magnets on the rack interfere with the stationary magnets, and the flux is routed internally. The connector is two-times axisymmetric and can dock at 0° and 180° offsets. It is not failsafe, as both sides must be actuated to decouple.

During coupling, two connectors are brought into contact with each other. The switching devices are active in their default position and can connect with the magnetic metal regions of the opposite connector. Data and power connections are established through IR transmitters and electrical contacts.

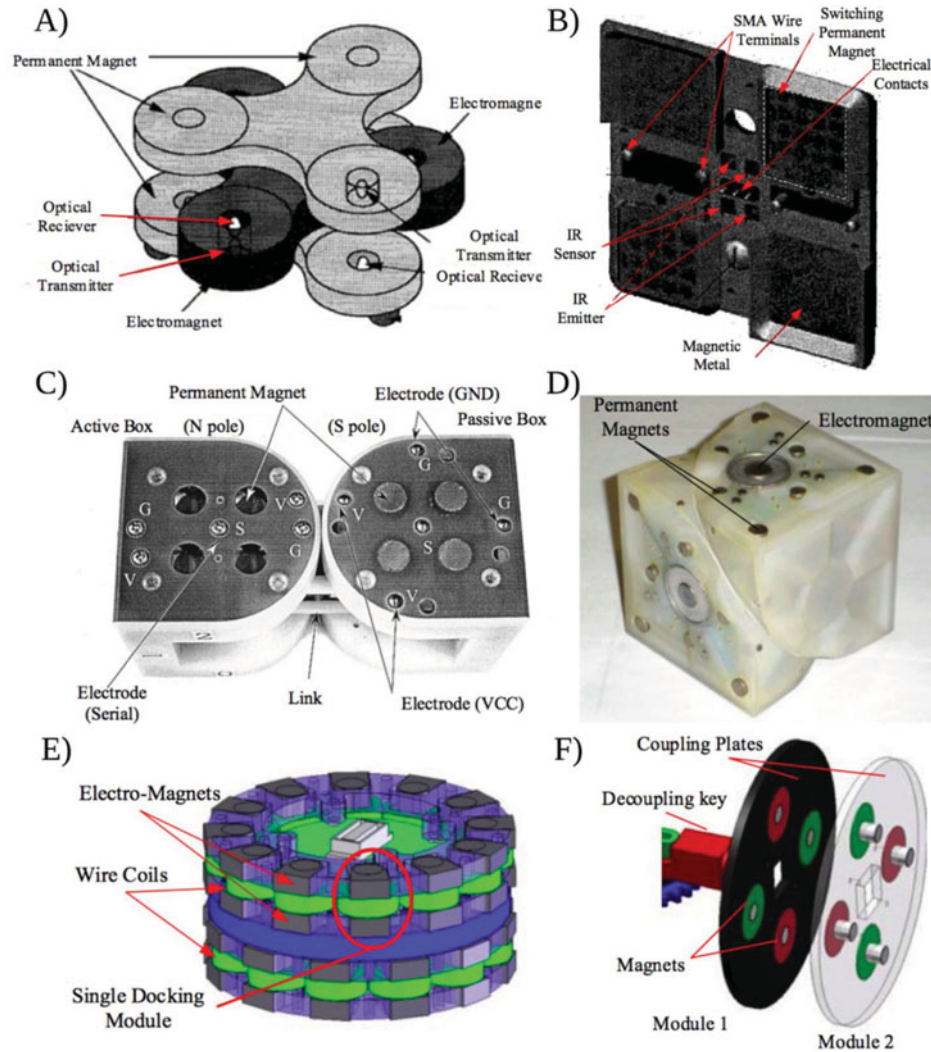


Fig. 8. Magnetic coupling mechanisms: (A) Design of Fractum robotic module, including electromagnet to permanent magnet docking system.^{65,66} (B) Coupling mechanism for the Telecubes robotic platform.^{67,68} (C) Coupling mechanism used on the M-TRAN I & II modular robots.^{69,70} (D) Molecubes module with connection surface.^{71–73} (E) CAD schematic of a Catoms robotic module.⁷⁴ (F) CAD schematic showing the coupling process of the SMORES mechanism. Modules approach and are coupled by permanent magnets.⁷⁵

To decouple, the SMA wire is actuated through Joule heating, and the switching devices are turned off. The modules are then free to move away and the connector can decouple, at which point the sliding racks return to the active position. Through the use of chamfered surfaces and materials with low coefficients of friction, the Telecubes coupling mechanism demonstrates a translational misalignment tolerance of $\pm N/A, 3, 3$ mm. The misalignment tolerance in the normal direction is not discussed, though the use of magnets implies that the connectors could likely be drawn together from a small distance.

5.3. M-TRAN I and II (2002-2003)

M-TRAN I and II^{70,71} utilize the gendered coupling mechanism shown in Fig. 8(C). The M-TRAN modules have dimensions $60 \text{ mm} \times 60 \text{ mm} \times 120 \text{ mm}$ and serve as building blocks that can reconfigure into different shapes. As shown in Fig. 8(C) the passive box has four permanent magnets mounted on the surface, and the active box has four permanent magnets embedded below the surface on a plate that is held down by a helical spring. A coil of SMA wire is attached between this plate and the surface of the connector. The M-TRAN I and II connector is four-times axisymmetric and can dock at 0° , 90° , 180° , and 270° offsets.

The coupling process begins when an active face is brought close to a passive face. The magnetic forces pull the interior magnets of the active connector up to its surface, compressing the springs and the SMA coil. The connection between the magnets provides about 25 N of holding force. Electric connections are made through the electrodes embedded in the surface, which are offset to allow for connections at any docking angle. To disconnect, the SMA coil is heated, causing it to push the inner plate back inside the body of the connector to a sufficient distance that the magnetic force is weakened and the connection breaks. In the latest generation of this modular robot, M-TRAN III, this coupling mechanism was replaced by a mechanical coupler, as was discussed in Section 4.2.6. The double-cube design of the M-TRAN was shown by its authors to be more efficient than a single-cube construction in terms of the amount of torque required to rearrange a module in a lattice. A self-reconfiguration planner was also implemented, in which lattice-distance is used as a metric to determine the difficulty of a given shape change.

5.4. Molecubes (2007)

A Molecubes module,^{72–74} shown in Fig. 8(D), is cubic in shape, with an edge length of 10 cm, and is split in two halves that can rotate along the diagonal plane. The docking system incorporated into the Molecubes robot consists of a large electromagnet in the center and four permanent magnets radiating from it in 90° intervals. There are also four permanent magnets located on the corners of the connector for increased strength. The surface of the connector has inset pockets and other alignment geometry. While the connection surface is four-times axisymmetric, it is not failsafe as both modules must be active to decouple.

During coupling, two surfaces are brought into contact with each other. The alignment features on the surfaces interconnect, and the permanent magnets hold the modules together. Without engaging the electromagnets, the permanent magnet connection can hold two cantilevered modules. To strengthen the bond, the electromagnets on the two modules can be set to opposite polarities. With the electromagnets engaged, the connection can hold three cantilevered modules. The connection is also strong enough to maintain 1.41 N·m of torque to rotate the connected modules. To disengage, the electromagnets of the two modules are set to the same polarities, pushing the modules apart.

5.5. Catoms (2007)

Claytronic atoms (Catoms)⁷⁵ use custom designed electromagnets as their coupling interface. As seen in Fig. 8(E), each Catom module is 45 mm in diameter and has 24 pairs of electromagnets arranged in two rings. The rings are offset by 15°, and the electromagnet pairs in each ring are offset by 30°. The electromagnets are trapezoidal in shape and have flat edges for interfacing with other modules. Because the coupling interface spans the entire circumference of the module, it is 24-times axisymmetric. This mechanism is failsafe, as switching the magnets of one module is all that is necessary for disengagement. As in the Fractum modules, the electromagnets in the Catoms modules are used for both coupling and planar locomotion of the units. Modules can move relative to each other by progressively switching their external magnets on and off, but cannot independently move.

To begin coupling, the magnets that are to be used to create the desired connection point are first identified on the two modules. The magnets are then energized with opposite polarities and are drawn together, aligning the modules in the process. At the beginning of the coupling procedure, the magnets generate a torque of about 12 mN·m at full power to rotate and align the Catom units. Once the magnets are flat against each other, they can generate 200 mN·m of torque when fully powered. To maintain the connection, the electromagnets must remain powered on.

5.6. SMORES (2012)

The Self-assembling MODular Robot for Extreme Shape-shifting (SMORES)⁷⁶ is another example of a modular robot that utilizes permanent magnets to establish connections. A SMORES module is 100 mm × 100 mm × 90 mm in size and features three active and one passive coupling plate. Two additional discs act as wheels, allowing an individual module to locomote and steer with differential drive. All of the connectors are actuated by independent DOFs. The active plates can be rotated by means of a gear motor, while the passive plates are stationary. The SMORES coupling mechanism is considered genderless if two active plates are connected, since both sides of the connection are identical. However, it is possible to connect an active plate with a passive plate, in which case the connection is considered gendered. As seen in Fig. 8(F), each coupling plate, passive or active, has

two positive and two negative permanent magnets embedded in the surface. Like many of the other coupling mechanisms discussed in this category, establishing a connection requires bringing the two connectors into proximity, which is then drawn together by the attractive forces between the opposing magnets. The connection can maintain 60 N of force in tension and can transmit up to 11 N-m in rotational torque.

An integral component of the SMORES modules is the decoupling mechanism. Inside each module, a decoupling key, shown in Fig. 8(F), is mounted on a central mechanism that can selectively extend the key outwards through any of the active surfaces. To decouple, the key is extended through the faces of both modules. First, the key fits into the square hole on the opposing module, while an indentation on the shaft allows the inner module to rotate. Then, by rotating the inner module, the magnets of similar polarities face each other and the connection is broken. The decoupling key can also be extended through the connectors to increase the strength of the bond. The SMORES coupling mechanism is structurally four-times axisymmetric, but because the active docking plates can rotate, it can be considered fully axisymmetric.

5.7. *M-Blocks (2015)*

The Momentum-driven, Magnetic Modular Robots (M-Blocks) module⁷⁷ is a cubic unit that employs 24 polarized magnets embedded in its edges (3 at each vertex) to allow both mating and pivoting interactions between adjacent modules. A flywheel located near one of the cube's faces is rapidly accelerated to exert a torque on the module, so that adjacent units mated along an edge can rotate with respect to each other in a hinge-like motion. Docking occurs when two full faces of adjacent modules come in contact, so that fully eight magnets in each module are in close proximity. Arranging magnets in a grid in this way improves mating robustness and maximizes misalignment tolerance by insuring that force is applied over the largest possible area. This setup also both enables two separate mating modes (face and edge), and allows for consistent elementary motions between modules that can be used to perform complex rearrangements in a lattice. Whereas most models of cubic modular robots interacting in a lattice assume that blocks move by sliding in one of the six directions normal to their faces, the pivoting motions used by M-Blocks are still able to produce general reconfiguration, while also allowing for new modalities, such as movement around sharp corners.

6. Comparative Analysis

In the previous sections, the designs of various coupling mechanisms implemented in modular reconfigurable robots were presented according to the classification scheme introduced in Section 3, with special focus on common design principles found in the literature. In this section, a cross-assessment of the design attributes discussed in Section 2 of each docking mechanism is presented in order to establish a comparative scheme that highlights critical aspects of the existing technologies.

In Table I, the coupling mechanisms discussed in this survey are organized according to the form factor of the system in which they were implemented. The year of invention, means of actuation, and symmetry of each mechanism are also presented in this table. The primary coupling elements incorporated on each interface are also presented, to provide an overview of the different design approaches adopted in different systems.

To provide a more holistic view of the work reviewed in this paper, Table II assigns selected design attributes of coupling mechanisms, specifically the gender and fail-safe criteria, to each connector. Moreover, the instrumentation/sensors incorporated into the coupling interfaces for alignment control and data/power sharing is also highlighted, where applicable. Among the solutions explored for these problems are the uses of IR, optical, and ultrasonic sensors, as well as the use of spring-loaded electric pins and other types of electric connectors, as indicated in the table below.

Misalignment tolerance is of particular importance in the field of modular robotics. The experimentally measured values of misalignment tolerance for coupling mechanisms reported in the literature are presented in Table III, using the convention presented in Section 2.4.

The information presented in these tables sheds light on some trends in the design of coupling mechanisms that have emerged as the field of modular robots has developed in the last two decades. For example, it can be seen in Table I that the miniature robots incorporate more mechanisms actuated by magnets and SMA wires, as compared to the macro-scale robots. Such mechanisms are more compact and are therefore preferable for modules of smaller size. Whereas larger modules may be intended

Table I. Overview of docking mechanisms: form factor, year of invention, coupling interface, symmetry, and actuation.

Form factor	Coupling mechanism	Year	Coupling interface	Symmetry (Deg.)	Actuation
Macro	CEBOT ^{33,34}	1988	Hooks	0, 180	Gear motor with worm gear
	Fractum ^{66,67}	1994	Perm. & elect. magnets	0, 120, 240	Electromagnetic
	3D self-reconfigurable ³⁶	1998	Hooks	0, 90, 270	Gear motor, non-back drivable worm gear
	CONRO ^{2,11,12}	2002	Pin & hole – latch	180	Gear motor, SMA
	Millibots ¹⁷	2000	Pin & hole – latch	asymmetric	SMA
	PolyBot G2 ^{13,16}	2002	Pin & hole – latch	0, 90, 180, 270	SMA
	Swarm-Bot ³⁸	2006	Hooks – gripper	full axisymmetry	Servomotor
	JL-1 ²²	2006	Pin & hole - latch	0, 180	Gear motor
	ATRON ^{39,40}	2004	Hooks		Gear motor
	Molecubes ⁷²	2007	Perm. & elect. magnets	0, 90, 180, 270	Electromagnetic
	JL-2 ⁴¹	2010	Hooks – gripper	0, 90, 180, 270	Gear motor
	Transmote ⁵⁵	2012	Lock & key		Gear motor
	RoGenSiD ⁶¹	2013	Shape match – rot. fingers	0, 90, 180, 270	Gear motor plus worm gear transmission (non-back drivable)
	Tristate ²⁷	2014	Pin & hole – clamps	0, 180	Gear motor plus worm gear transmission (non-back drivable)
Miniature	Trimobot ⁵⁰	2015	Hooks	0, 180	Gear motor
	GHEFT ⁶⁴	2016	Shape match – clamps	0, 180	Servo motors driving a constant lead CAM, worm gear transmission (non-back drivable)
	Crystalline ⁵¹	2001	Lock & key	0, 180	Gear motor
	I-cubes ⁵³	2001	Lock & key	0, 90, 180, 270	Servomotor
	Dragon ¹⁹	2002	Pin & hole – latch	0, 90, 270	Gear motor, SMA
	Telecubes ⁶⁸	2002	Switching perm. magnets	0, 180	SMA
	M-TRAN I and II ⁷¹	2003	Perm. magnets	0, 90, 180, 270	Magnetic, SMA, non-back drivable
	Catoms ⁷⁵	2007	Elect. magnets	24-times axisymmetric	Electromagnetic
	M-TRAN III ⁴²	2008	Hooks	0, 90, 180, 270	Gear motor
	SINGO ⁵⁷	2009	Shape match - linear fingers	0, 90, 180, 270	Gear motor, non-back drivable circular gearing
	Roombots ⁴⁴	2010	Hooks	0, 90, 180, 270	Gear motor
	SAMBOT ⁴⁷	2011	Hooks	0, 180	Gear motor
	GENFA ²³	2011	Pin & hole - latch	0, 90, 180, 270	Gear motor, non-back drivable worm gear
	SMORES ⁷⁶	2012	Perm. magnet	0, 90, 180, 270	Magnetic, gear motor
	Micro self-reconfigurable ²⁵	2013	Pin & hole - latch	0, 180	SMA
	HiGen ⁶³	2014	Shape match - rot. fingers	0, 90, 180, 270	Gear motor plus worm gear transmission (non-back drivable)

Table II. Design attributes of docking mechanisms: gender, failsafe criteria, alignment sensors, and data sharing capabilities.

Robot platform or coupling mechanism	Gender	Failsafe (Y/N)	Alignment sensors	Data sharing capabilities
CEBOT ^{32–34}	Gendered	N	IR	Electric contacts*
Fractum ^{66,67}	Gendered	N	IR	IR
3D Self-Reconfigurable ^{35,36}	Bi-gendered	N	–	–
CONRO ^{2,11,12}	Gendered	N	IR	IR
Millibots ^{17,18}	Gendered	N	–	–
PolyBot G2 ^{13,14}	Bi-gendered	N	IR	Electric contacts*
Swarm-Bot ^{37,38}	Gendered	N	IR, Light sensors	–
JL-I ^{20–22}	Gendered	N	–	–
ATRON ^{39,40}	Gendered	N	IR	IR
Molecubes ^{72–74}	Gendered	N	–	Electric contacts*
JL-II ⁴¹	Gendered	N	Sonar	–
Transmote ⁵⁵	Gendered	N	IR	–
RoGenSiD ⁶¹	Genderless	Y	–	Electric contacts*
Tristate ^{27–29}	Gendered	N	–	–
Trimobot ⁵⁰	Gendered	N	IR, Camera	–
GHEFT ^{64,65}	Genderless	Y	–	–
Crystalline ^{51,52}	Gendered	N	–	–
I-Cubes ^{53,54}	Gendered	N	–	–
DRAGON ^{9,19}	Bi-gendered	N	IR	IR, electric contacts*
Telecubes ^{68,69}	Bi-gendered	N	IR	Electric contacts*
M-TRAN I and II ^{70,71}	Gendered	N	IR	Electric contacts
Catoms ⁷⁵	Genderless	Y	IR	IR/inductive*
M-TRAN III ^{42,43}	Gendered	N	IR, Camera	Electric contacts
SINGO ⁵⁷	Genderless	Y	–	–
Roombots ^{44–46}	Bi-gendered	N	–	–
SAMBOT ^{47–49}	Gendered	N	IR	Electric contacts*
GENFA ²³	Genderless	Y	IR	Electric contacts*
SMORES ⁷⁶	Genderless	N	–	–
Micro self-reconfigurable ^{25,26}	Gendered	N	–	–
HiGen ⁶³	Genderless	Y	–	Electric contacts*
M-Blocks ⁷⁷	Gendered	N	IR, Hall Effect	–

*Couplers equipped with power sharing capabilities.

for use in mobile configurations (legged robots, snakes, wheeled-vehicles, etc.), smaller modules are often intended for lattice-configurations and applications that may require less mobility. One such example is the notion of “claytronics,” in which large numbers of small, possibly microscopic, modules arrange themselves in order to produce macroscopic visual or physical properties, so called “physical rendering.” The need for individual modules to be fully mobile may also be decreased in such cases, as the combination of modules may still be quite small, and exterior electromagnetic forces or other means of manipulation may be used effectively. Other applications, such as modular variants of miniature sensors known as “smartdust,” may also be of use in passive or immobile capacities.

With reference to the year of invention in Table I, it is worth noting that while earlier coupling mechanisms used mechanical latches, typically within a pin-and-hole mechanism, the connectors developed within the last decade deviated from this design principle and opted for other docking methods using hooks, lock-and-key designs, and shape-matching profiles. This design choice can be attributed to the recent developments of more compact mechanical actuators, which are necessary for this kind of application. However, the shift away from pin-and-hole connectors also reflects several deficiencies in their performance. Such connectors are bi-gendered at best and typically require actuation from both sides of the connection; the pins must be inserted in the holes and then the latches engaged in a subsequent step, as seen in several examples discussed in Section 4.1. Meanwhile, hooks and grippers, as well as lock-and-key connectors, usually require a single motion to establish the connection, simplifying the docking process. Table II shows that shape-matching coupling

Table III. Reported misalignment tolerance data.

Coupling mechanism	Year	Misalignment tolerance					
		$\pm X$ (mm)	$\pm Y$ (mm)	$\pm Z$ (mm)	$\pm \beta^\circ$	$\pm \gamma^\circ$	$\pm \alpha^\circ$
PolyBot G2 ^{13,14}	2002	0	3	3	8	8	8
DRAGON ^{9,19}	2002	0	15	15	45	45	45
Telecubes ^{68,69}	2002	–	3	3	–	–	–
JL-I ^{20–22}	2006	30	30	30	45	45	45
M-TRAN III ⁴²	2008	2	5	5	10	10	10
SINGO ⁵⁷	2009	6	5	5	22	5	5
JL-II ⁴¹	2010	2	5	5	10	10	10
SAMBOT ^{47–49}	2011	13	4.5	19.5	5	5	10
Transmote ⁵⁵	2012	0	30	30	–	15	15
RoGenSiD ⁶¹	2013	20	2	2	2.4	2.4	2.4
HiGen ⁶³	2014	13.5	2.5	2.5	8	8	10
GHEFT ^{64,65}	2016	6	28	11	45	13	11

mechanisms, such as GHEFT, GENFA, SINGO, HiGen, and RoGenSid, are typically genderless. This enables higher levels of robustness during the self-reconfiguration procedure, since modules can establish connections at arbitrary coupling interfaces without gender constraints. It can also be seen in Table II that genderless mechanisms are mostly failsafe, which explains the increased interest in developing such mechanisms. Despite recent developments of new sensor technologies, IR sensors are chosen almost exclusively for alignment purposes. It is also evident that there has recently been increased interest both in power sharing technologies, which increase the overall energy-efficiency of the system, and the tolerance for misalignment, as indicated by Tables II and III. Designs with fewer DOF tend to compensate for their reduced ability to accurately position their docking-mechanisms by employing devices with higher misalignment tolerances, and vice versa.

7. Conclusion

This paper reviewed key research contributions to the methods and design principles of modular robotic coupling. The critical design attributes of gender status, axisymmetry, and misalignment tolerance were presented for each mechanism, allowing for a comparison of each mechanism's performance and robustness. A classification scheme was proposed that comprised of two categories: mechanical couplers and magnetic couplers. The mechanical couplers were further subcategorized according to the design approach and the types of mechanical elements involved in the connections.

The discussion of the couplers presented in the previous sections highlights some critical limitations of current coupling mechanism technology. Mechanical couplers with small hooks or pins are potentially vulnerable to abrupt impact forces, while claw-like connections may not ensure rigidity in all directions. Work also remains in ensuring the reliability of mechanisms using magnetic connections or SMA latches. A secure connection between modules is required to ensure predictable interaction of adjacent modules, maintain the functionality of the whole robot in variable conditions, and maximize the number of modules that can be docked in a specific formation. Ensuring that mechanical connectors are rigid and do not fail under abrupt impact is thus critical if modular robots are to reach their full potential in applications dealing with unstructured environments and unpredicted events. To promote the overall robotic system's robustness, the coupling mechanisms also need to be failsafe, a feature found in only a few of the mechanisms discussed here, as Table II demonstrates. With non-failsafe coupling, a robotic structure of potentially tens of modules could possibly fail because of one failed connection or faulty module. Last, a truly adaptable robot must have a substantial tolerance for misalignment. About half of the mechanisms presented in Table III have misalignment tolerances of 10° or less in at least one direction.

Several guidelines for designers and some promising directions for future research are also evident from the literature. Coupling mechanisms should be chosen for their probable application, as in the robust, high-torque coupler used in the mobile JL-series of robots, or (on the opposite side of the spectrum), the compact but numerous magnets used in the immobile Catoms units. M-blocks point

a way forward with magnetic coupling, with their use of multiple magnets enabling extra coupling-strength and redundancy, multiple coupling-modes, and new lattice-motion modalities. Modular units in a reconfigured state should attempt to maximize their maneuverability to maximize the probability of making a strong connection. The Swarm-bot's use of a flexible manipulator and full axisymmetry demonstrate a promising approach, which also gave groups of mated robots a helpful source of extra flexibility and mutual-manipulation. An alternate approach is to compensate for fewer DOFs with an increase in axisymmetry and misalignment tolerance of the docking mechanism, as a wide variety of the presented examples successfully demonstrate. Rather than designing a dichotomy of mobile versus lattice-type modular robots, the use of meta-modules, as in the ATRON, Roombots, and Crystalline systems, can be used to fill the gap in between, with a hierarchy of locomotion modalities providing a complementary range of locomotion and manipulation abilities. The M-Tran robots emphasize the importance of module shape in maximizing the efficiency and usability of the full system. Finally, the Crystalline system's use of compressibility in 3-D lattice algorithms suggests that the full potential of these systems will be realized by the use of cooperative behavior between many modules, rather than requiring that modules always move independently.

Robust and reversible coupling mechanisms are of central importance to the field of modular robotics. Despite numerous achievements, several challenges still lie ahead in terms of the rigidity and overall reliability of the connections. Addressing these issues will require novel approaches to coupling mechanism design that are simultaneously rigid, reversible, non-back drivable, and failsafe. The authors hope that the material presented in this paper will provide a better understanding of the current status of robotic coupling technologies and will facilitate further innovation in this field.

Acknowledgements

The authors would like to thank Brock Davis for helping catalog existing literature on coupling mechanisms and Youssef Haridy for editing this paper.

References

1. M. Yim, Y. Zhang and D. Duff, "Modular robots," *IEEE Spectr.* **39**(2), 30–34 (2002).
2. A. Castano, W. Shen and P. Will, "CONRO: Towards deployable robots with inter-robot metamorphic capabilities," *Auton. Robots.* **8**(3), 309–324 (2000).
3. J. Feczko, M. Manka, P. Krol, M. Giergiel, T. Uhl and A. Pietrzyk, "Review of the Modular Self Reconfigurable Robotic Systems," Proceedings of the *IEEE International Workshop on Robot Motion and Control*, Poznan, Poland (2015) pp. 182–187.
4. P. Moubarak and P. Ben-Tzvi, "Modular and reconfigurable mobile robotics," *Rob. Auton. Syst.* **60**(12), 1648–1663 (2012).
5. W. Fehse, "Automated Rendezvous and Docking of Spacecraft," (Cambridge University Press, 2003).
6. W. X. C. Z. S. Chengxun and Z. Qingrui, "Docking dynamics of a spacecraft," *J. Astronaut.* **3**, 15–24 (1991).
7. R. Stokey, M. Purcell, N. Forrester, T. Austin, R. Goldsborough, B. Allen and C. von Alt, "A Docking System for REMUS, An Autonomous Underwater Vehicle," Proceedings of the *MTS/IEEE Conference Proceedings Ocean*, Halifax, Canada (1997) pp. 1132–1136.
8. S. Cowen, S. Briest and J. Dombrowski, "Underwater Docking of Autonomous Undersea Vehicles Using Optical Terminal Guidance," Proceedings of the *MTS/IEEE Conference Proceedings Ocean*, Halifax, Canada (1997) pp. 1143–1147.
9. M. Nilsson, "Heavy-Duty Connectors for Self-Reconfiguring Robots," Proceedings of the *IEEE International Conference on Robotics and Automation*, Washington, DC (2002).
10. S. Murata, E. Yoshida, H. Kurokawa, K. Tomita and S. Kokaji, "Self-repairing mechanical systems," *Auton. Robots.* **10**(1), 7–21 (2001).
11. A. Castano, A. Behar and P. M. Will, "The Conro modules for reconfigurable robots," *IEEE/ASME Trans. Mechatronics.* **7**(4), 403–409 (2002).
12. M. Rubenstein, K. Payne, P. Will, W.-M. S. W.-M. Shen, "Docking Among Independent and Autonomous CONRO Self-Reconfigurable Robots," Proceedings of the *IEEE International Conference on Robotics and Automation*, New Orleans, LA (2004) pp. 2877–2882.
13. M. Yim, Y. Zhang, K. Roufas, D. Duff and C. Eldershaw, "Connecting and disconnecting for chain self-reconfiguration with PolyBot," *IEEE/ASME Trans. Mechatronics.* **7**(4), 442–451 (2002).
14. M. Yim, K. Roufas, D. Duff, Y. Zhang, C. Eldershaw and S. Homans, "Modular reconfigurable robots in space applications," *Auton. Robots.* **14**(2), 225–237 (2003).
15. M. Yim, "Locomotion with a Unit-Modular Reconfigurable Robot," Stanford University, Stanford, CA, USA, 1994.

16. M. Yim, D. G. Duff and K. D. Roufas, "PolyBot: A Modular Reconfigurable Robot," *Proceedings of the IEEE International Conference on Robotics and Automation*, San Francisco, CA (2000) pp. 514–520.
17. H. B. Brown, J. M. Vande Weghe, C. A. Bererton, and P. K. Khosla, "Millibot trains for enhanced mobility," *IEEE/ASME Trans. Mechatronics*. **7**(4), 452–461 (2002).
18. R. Grabowski, P. Khosla and H. Choset, "Development and Deployment of a Line of Sight Virtual Sensor for Heterogeneous Teams," *Proceedings of the IEEE International Conference on Robotics and Automation*, New Orleans, LA (2004) pp. 3024–3029.
19. M. Nilsson, "Connectors for self-reconfiguring robots," *IEEE/ASME Trans. Mechatronics*. **7**(4), 473–474 (2002).
20. G. Zong, Z. Deng and W. Wang, "Realization of a Modular Reconfigurable Robot for Rough Terrain," *Proceedings of the IEEE International Conference on Mechatronics and Automation*, Henan, China (2006) pp. 289–294.
21. H. X. Zhang, S. Y. Chen, W. Wang, J. W. Zhang, and G. H. Zong, "Runtime Reconfiguration of a Modular Mobile Robot with Serial and Parallel Mechanisms," *Proceedings of the IEEE/RSJ International Conference on Intelligent Robots and Systems*, San Diego, CA (2007) pp. 2999–3004.
22. H. Zhang, Z. Deng, W. Wang, J. Zhang and G. Zong, "Locomotion Capabilities of a Novel Reconfigurable Robot with 3 DOF Active Joints for Rugged Terrain," *Proceedings of the IEEE/RSJ International Conference on Intelligent Robots and Systems*, Beijing, China, (2006) pp. 5588–5593.
23. G. Fu, A. Menciassi and P. Dario, "Development of a Genderless and Fail-Safe Connection System for Autonomous Modular Robots," *Proceedings of the IEEE International Conference on Robotics and Biomimetics*, Phuket, Thailand (2011) pp. 877–882.
24. S. Kernbach, E. Meister, F. Schlachter, K. Jebens, M. Szymanski, J. Liedke, D. Laneri, L. Winkler, T. Schmickl and R. Thenius, "Symbiotic Robot Organisms: REPLICATOR and SYMBRION Projects," *Proceedings of the 8th Workshop on Performance Metrics for Intelligent Systems*, Gaithersburg, MD (2008) pp. 62–69.
25. E. Yoshida, A. I. Sci and A. I. Scie, "Micro self-reconfigurable modular robot using shape memory alloy micro self-reconfigurable modular robot using shape memory alloy," *Distrib. Auton. Robot. Syst.* **4**(2), 212–218 (2013).
26. L. E. Parker, G. Bekey and J. Barhen, "Distributed autonomous robotic systems," *J. Chem. Inf. Model.* **53**(9), 1689–1699 (2013).
27. P. M. Moubarak and P. Ben-Tzvi, "A tristate rigid reversible and non-back-drivable active docking mechanism for modular robotics," *IEEE/ASME Trans. Mechatronics*. **19**(3), 840–851 (2014).
28. P. M. Moubarak, P. Ben-Tzvi, Z. Ma, and E. J. Alvarez, "An Active Coupling Mechanism with Three Modes of Operation for Modular Mobile Robotics," *Proceedings of the IEEE International Conference on Robotics and Automation*, Karlsruhe, Germany (2013) pp. 5489–5494.
29. P. M. Moubarak and P. Ben-Tzvi, "On the dual-rod slider rocker mechanism and its applications to tristate rigid active docking," *J. Mech. Robot.* **5**(1), 11010 (2013).
30. P. M. Moubarak, E. J. Alvarez and P. Ben-Tzvi, "Reconfiguring a Modular Robot into a Humanoid Formation: A Multi-Body Dynamic Perspective on Motion Scheduling for Modules and Their Assemblies," *Proceedings of the IEEE International Conference on Automation Science and Engineering*, Madison, WI (2013) pp. 687–692.
31. P. Kumar, W. Saab and P. Ben-Tzvi, "Design of a Multi-Directional Hybrid-Locomotion Modular Robot with Feedforward Stability Control," *Proceedings of the ASME International Design Engineering Technical Conferences and Computers and Information in Engineering Conference*, Cleveland, OH (2017).
32. T. Fukuda, M. Buss, H. Hosokai and Y. Kawauchi, "Cell structured robotic system CEBOT: Control, planning and communication methods," *Rob. Auton. Syst.* **7**(2–3), 239–248 (1991).
33. T. Fukuda, T. Ueyama, Y. Kawauchi and F. Arai, "Concept of Cellular Robotic System (CEBOT) and basic strategies for its realization," *Comput. Electr. Eng.* **18**(1), 11–39 (1992).
34. T. Fukuda, S. Nakagawa, Y. Kawauchi and M. Buss, "Self Organizing Robots Based on Cell Structures – CEBOT," *Proceedings of the IEEE International Workshop on Intelligent Robots*, Scottsdale, AZ (1988) pp. 145–150.
35. E. Yoshida, S. Murata, A. Kamimura and K. Tomita, "Self-Reconfigurable Modular Robots-Hardware and Software Development in AIST," *Proceedings of the IEEE International Conference on Robotics, Intelligent Systems and Signal Processing*, Hunan, China (2003) pp. 339–346.
36. S. Murata, H. Kurokawa, E. Yoshida, K. Tomita and S. Kokaji, "A 3-D Self-Reconfigurable Structure," *Proceedings of the IEEE/RSJ International Conference on Intelligent Robots and Systems*, Victoria, Canada (1998).
37. F. Mondada, L. M. Gambardella, D. Floreano, S. Nolfi, J. L. Deneubourg and M. Dorigo, "The cooperation of swarm-bots: Physical interactions in collective robotics," *IEEE Robot. Autom. Mag.* **12**(2), 21–28 (2005).
38. R. Groß, M. Bonani, F. Mondada and M. Dorigo, "Autonomous Self-Assembly in a Swarm-Bot," *Proceedings of the 3rd International Symposium on Autonomous Minirobots for Research and Edutainment*, Berlin, Heidelberg (2006) pp. 314–322.
39. M. W. Jorgensen, E. H. Ostergaard and H. H. Lund, "Modular ATRON: Modules for a Self-Reconfigurable Robot," *Proceedings of the IEEE/RSJ International Conference on Intelligent Robots and Systems*, Sendai, Japan, 40AD, pp. 2068–2073.
40. E. H. Østergaard, K. Kassow, R. Beck and H. H. Lund, "Design of the ATRON lattice-based self-reconfigurable robot," *Auton. Robots.* **21**(2), 165–183 (2006).

41. W. Wang, W. Yu and H. Zhang, "JL-2: A mobile multi-robot system with docking and manipulating capabilities," *Int. J. Adv. Robot. Syst.* **7**(1), 9–18 (2010).
42. H. Kurokawa, K. Tomita, A. Kamimura, S. Kokaji, T. Hasuo and S. Murata, "Distributed self-reconfiguration of M-TRAN III modular robotic system," *Int. J. Rob. Res.* **27**(3–4), 373–386 (2008).
43. S. Murata, K. Kakomura and H. Kurokawa, "Docking Experiments of a Modular Robot by Visual Feedback," *Proceedings of the IEEE/RSJ International Conference on Intelligent Robots and Systems*, Beijing, China (2006).
44. A. Spröwitz, S. Pouya, S. Bonardi, J. Van Den Kieboom, R. Möckel, A. Billard, P. Dillenbourg and A. Ijspeert, "Roombots: Reconfigurable robots for adaptive furniture," *IEEE Comput. Intell. Mag.* **5**(3), 20–32 (2010).
45. A. Sproewitz, M. Asadpour, A. Billard, P. Dillenbourg and J. Ijspeert, "Roombots–Modular Robots for Adaptive Furniture," *Proceedings of the IEEE/RSJ International Conference on Intelligent Robots and Systems*, Nice, France (2008).
46. A. Sproewitz, A. Billard, P. Dillenbourg and A. J. Ijspeert, "Roombots–Mechanical Design of Self-Reconfiguring Modular Robots for Adaptive Furniture," *Proceedings of the IEEE International Conference on Robotics and Automation*, Kobe, Japan (2009) pp. 4259–4264.
47. H. Wei, Y. Chen, J. Tan and T. Wang, "Sambot: A self-assembly modular robot system," *IEEE/ASME Trans. Mechatronics.* **16**(4), 745–757 (2011).
48. H.-X. Wei, H.-Y. Li, Y. Guan and Y.-D. Li, "A dynamics based two-stage path model for the docking navigation of a self-assembly modular robot (Sambot)," *Robotica.* **34**(7), 1517–1528 (2016).
49. H. Wei, D. Li, J. Tan and T. Wang, "The Distributed Control and Experiments of Directional Self-Assembly for Modular Swarm Robots," *Proceedings of the IEEE/RSJ International Conference on Intelligent Robots and Systems*, Taipei, Taiwan (2010) pp. 4169–4174.
50. Y. Zhang, G. Song, S. Liu, G. Qiao, J. Zhang and H. Sun, "A modular self-reconfigurable robot with enhanced locomotion performances: design, modeling, simulations, and experiments," *J. Intell. Robot. Syst.* **81**(3–4), 377–393 (2016).
51. M. V. D. Rus, "Self-Reconfiguration with compressible unit modules," *J. Auton. Robot.* **10**(1), 107–124 (2001).
52. R. Fitch, D. Rus and M. Vona, "A basis for self-repair robots using self-reconfiguring crystal modules," *Intell. Auton. Syst.* **6**, 903–910 (2000).
53. P. K. Khosla, "A modular self-reconfigurable bipartite robotic system: Implementation and motion planning," *Auton. Robots.* **10**(1), 23–40 (2001).
54. C. Unsal and P. K. Khosla, "A Multi-Layered Planner for Self-Reconfiguration of a Uniform Group of I-Cube Modules," *Proceedings of the IEEE/RSJ International Conference on Intelligent Robots and Systems*, Maui, HI (2001) pp. 598–605.
55. G. Qiao, G. Song, J. Zhang, H. Sun, W. Wang and A. Song, "Design of transmute: A Modular Self-Reconfigurable Robot with Versatile Transformation Capabilities," *Proceedings of the IEEE International Conference on Robotics and Biomimetics*, Guangzhou, China (2012) pp. 1331–1336.
56. G. Qiao, G. Song, Y. Wang, J. Zhang and W. Wang, "Autonomous network repairing of a home security system using modular self-reconfigurable robots," *IEEE Trans. Consum. Electron.* **59**(3), 562–570 (2013).
57. W. M. Shen, R. Kovac and M. Rubenstein, "Singo: A Single-End-Operative and Genderless Connector for Self-Reconfiguration, Self-Assembly and Self-Healing," *Proceedings of the IEEE International Conference on Robotics and Automation*, Kobe, Japan (2009) pp. 4253–4258.
58. B. Salemi, M. Moll and W. M. Shen, "SUPERBOT: A Deployable, Multi-Functional, and Modular Self-Reconfigurable Robotic System," *Proceedings of the IEEE/RSJ International Conference on Intelligent Robots and Systems*, Beijing, China (2006) pp. 3636–3641.
59. W.-M. Shen, M. Krivokon, H. Chiu, J. Everist, M. Rubenstein and J. Venkatesh, "Multimode locomotion via superbot reconfigurable robots," *Auton. Robots.* **20**(2), 165–177 (2006).
60. W.-M. Shen, M. Krivokon, H. Chiu, J. Everist, M. Rubenstein and J. Venkatesh, "Multimode Locomotion via Superbot Robots," *Proceedings of the IEEE International Conference on Robotics and Automation*, Orlando, FL (2006) pp. 2552–2557.
61. S. G. M. Hossain and C. A. Nelson, "RoGenSiD: A Rotary Plate Genderless Single-Sided Docking Mechanism for Modular Self-Reconfigurable Robots," *Proceedings of the ASME International Design Engineering Technical Conferences and Computers and Information in Engineering Conference*, Portland, OR (2013) pp. 1–7.
62. J. Baca, S. G. M. Hossain, P. Dasgupta, C. A. Nelson and A. Dutta, "Modred: Hardware design and reconfiguration planning for a high dexterity modular self-reconfigurable robot for extra-terrestrial exploration," *Rob. Auton. Syst.* **62**(7), 1002–1015 (2014).
63. C. Parrott, T. J. Dodd and R. Grob, "HiGen: A High-Speed Genderless Mechanical Connection Mechanism with Single-Sided Disconnect for Self-Reconfigurable Modular Robots," *Proceedings of the IEEE/RSJ International Conference on Intelligent Robots and Systems*, Chicago, IL (2014) pp. 3926–3932.
64. W. Saab and P. Ben-Tzvi, "Development of a Novel Coupling Mechanism for Modular Self-Reconfigurable Mobile Robots," *Proceedings of the ASME International Design Engineering Technical Conferences and Computers and Information in Engineering Conference*, Boston, Ma (2015) p. V05BT08A007.
65. W. Saab and P. Ben-Tzvi, "A genderless coupling mechanism with six-degrees-of-freedom misalignment capability for modular self-reconfigurable robots," *J. Mech. Robot.* **8**(6), (2016).

66. K. Tomita, S. Murata, H. Kurokawa, E. Yoshida and S. Kokaji, "Self-Assembly and self-repair method for a distributed mechanical system," *IEEE Trans. Robot. Autom.* **15**(6), 1035–1045 (1999).
67. S. Murata, H. Kurokawa and S. Kokaji, "Self-Assembling Machine," *Proceedings of the IEEE International Conference on Robotics and Automation*, San Diego, CA (1994) pp. 441–448.
68. J. W. Suh, S. B. Homans and M. Yim, "Telecubes: Mechanical Design of a Module for Self-Reconfigurable Robotics," *Proceedings of the IEEE International Conference on Robotics and Automation*, Washington, DC (2002) pp. 4095–4101.
69. S. Vassilvitskii, M. Yim and J. Suh, "A Complete, Local and Parallel Reconfiguration Algorithm for Cube Style Modular Robots," *Proceedings of the IEEE International Conference on Robotics and Automation*, Washington, DC (2002) pp. 117–122.
70. S. Murata, E. Yoshida, A. Kamimura, H. Kurokawa, K. Tomita and S. Kokaji, "M-TRAN: Self-Reconfigurable modular robotic system," *IEEE/ASME Trans. Mechatronics.* **7**(4), 431–441 (2002).
71. H. Kurokawa, A. Kamimura, E. Yoshida, K. Tomita, S. Kokaji and S. Murata, "M-TRAN II: Metamorphosis from a Four-Legged Walker to a Caterpillar," *Proceedings of the International Conference on Intelligent Robots and Systems*, Las Vegas, NV (2003) pp. 2454–2459.
72. V. Zykov, E. Mytilinaios, M. Desnoyer and H. Lipson, "Evolved and designed self-reproducing modular robotics," *IEEE Trans. Robot.* **23**(2), 308–319 (2007).
73. V. Zykov, A. Chan and H. Lipson, "Molecubes: An Open-Source Modular Robotics Kit," *Proceedings of the IEEE/RSJ International Conference on Intelligent Robots and Systems*, (2007) pp. 3–6.
74. V. Zykov, W. Phelps, N. Lassabe and H. Lipson, "Molecubes Extended: Diversifying Capabilities of Open-Source Modular Robotics," *Proceedings of the IEEE/RSJ International Conference on Intelligent Robots and Systems*, (2008) pp. 22–26.
75. B. T. Kirby, B. Aksak, J. D. Campbell, J. F. Hoberg, T. C. Mowry, P. Pillai and S. C. Goldstein, "A Modular Robotic System Using Magnetic Force Effectors," *Proceedings of the IEEE/RSJ International Conference on Intelligent Robots and Systems*, San Diego, CA (2007) pp. 2787–2793.
76. J. Davey, N. Kwok and M. Yim, "Emulating Self-Reconfigurable Robots – Design of the SMORES System," *Proceedings of the IEEE/RSJ International Conference on Intelligent Robots and Systems*, (2012) pp. 4464–4469.
77. J. W. Romanishin, K. Gilpin and D. Rus, "M-Blocks: Momentum-Driven, Magnetic Modular Robots," *Proceedings of the IEEE International Conference on Intelligent Robots and Systems*, (2013) pp. 4288–4295.